

# ERROR ANALYSIS OF ZFP COMPRESSION FOR FLOATING-POINT DATA\*

JAMES DIFFENDERFER<sup>†</sup>, ALYSON FOX<sup>‡</sup>, JEFFREY HITTINGER<sup>§</sup>, GEOFFREY SANDERS<sup>¶</sup>, AND PETER LINDSTROM<sup>||</sup>

**Abstract.** Compression of floating-point data will play an important role in high-performance computing as data bandwidth and storage become dominant costs. Lossy compression of floating-point data is powerful, but theoretical results are needed to bound its errors when used to store look-up tables, simulation results, or even the solution state during the computation. In this paper, we analyze the round-off error introduced by ZFP, a lossy compression algorithm. The stopping criteria for ZFP depends on the compression mode specified by the user; either fixed rate, fixed accuracy, or fixed precision [16]. While most of our discussion is focused on the fixed precision mode of ZFP, we establish a bound on the error introduced by all three compression modes. In order to tightly capture the error, we first introduce a vector space that allows us to work with binary representations of components. Under this vector space, we define operators that implement each step of the ZFP compression and decompression to establish a bound on the error caused by ZFP. To conclude, numerical tests are provided to demonstrate the accuracy of the established bounds.

**Key words.** Lossy compression, floating-point representation, error bounds

**AMS subject classifications.** 65G30, 65G50, 68P30

**1. Introduction.** For several reasons, the trade-offs to obtain high performance in computing have shifted. Traditionally, the emphasis on algorithmic complexity in numerical computation has focused on operation counts, which was justifiable when processor clock rates were increasing and memory was cheap and plentiful. With the end of Dennard scaling [6], clock speeds have frozen (or even reduced), so more capability, in terms of FLOPs, is now being obtained by adding more processing units [3]. Simultaneously, the ubiquity of hand-held devices and the power requirements of extreme-scale supercomputers is encouraging a shift to lower-power processors and co-processors.

Unfortunately, advances in memory and memory bandwidth are not increasing apace with the advances in processors. Thus, the memory per core and the bandwidth per core are decreasing as the number of processing units increases [4, 1]. The on-node cost of data motion (cache and main memory accesses), both in time and power, is increasingly the limiting factor in many calculations [4, 22]. Since off-node and I/O data motion have historically been orders of magnitude slower than on-node data motion, the movement of data anywhere on a computer system must now be seriously considered as the leading-order cost.

An obvious approach to address this challenge would be to consider data compression techniques. Indeed, lossless data compression is routinely used in network communications. However, for floating-point data typical of the scientific calculations done on high performance computers, standard lossless compression techniques such as Lempel–Ziv [23, 24], DEFLATE [7, 10], Lempel–Ziv–Welch [21], fzip [17] and other variants, which reproduce the original data with no degradation, struggle to produce significant compression rates [20, 17]. Lossy compression algorithms for floating-point data, e.g., SZ [8] and ZFP [14], allow an inexact approximation of the original data to be reconstructed from the compressed data. Lossy data compression typically produces a much higher rate of data reduction than lossless compression at the cost of introducing additional approximation error into the data.

\*Submitted to the editors 25 January 2018.

**Funding:** This work was performed under the auspices of the U.S. Department of Energy by Lawrence Livermore National Laboratory under Contract DE-AC52-07NA27344 and was supported by the LLNL-LDRD Program under Project No. 17-SI-004, LLNL-JRNL-744818-DRAFT.

<sup>†</sup>The University of Florida, Gainesville, FL ([jdiffer1@ufl.edu](mailto:jdiffer1@ufl.edu))

<sup>‡</sup>Lawrence Livermore National Laboratory, Livermore, CA ([fox33@llnl.gov](mailto:fox33@llnl.gov))

<sup>§</sup>Lawrence Livermore National Laboratory, Livermore, CA ([hittinger1@llnl.gov](mailto:hittinger1@llnl.gov))

<sup>¶</sup>Lawrence Livermore National Laboratory, Livermore, CA ([sanders29@llnl.gov](mailto:sanders29@llnl.gov))

<sup>||</sup>Lawrence Livermore National Laboratory, Livermore, CA ([lindstrom2@llnl.gov](mailto:lindstrom2@llnl.gov))

Lossy floating-point compression may be a useful tool in reducing data motion costs, particularly if there is a schema that allows for progressive (cf. global) decompression of data on demand. Certainly, for storage (e.g., tabular data) and I/O operations (data and restart files), there may be much to gain by using lossy compression provided that the data retain sufficient accuracy for the intended purposes. We propose that, in addition, solution state data in a simulation could be stored in a compressed state and be decompressed, operated on, and recompressed in a lossy way inline during each time step or iteration of a numerical algorithm. Numerical simulation is fundamentally about approximation, and the solution state already contains truncation, iteration, and other roundoff errors. However, the repeated application of compression and decompression does generate an additional error, and it must be shown that these lossy compression errors can be bounded to prove that such a process is stable.

As a first step towards this goal, we consider the ZFP lossy compression algorithm and develop an approach to analyze and bound the error resulting from lossy compression and decompression. While recent works have provided empirical studies of ZFP and other lossy compression algorithms on real-world data sets [2, 13, 15], this paper establishes the first closed form expression for bounds on the error introduced by ZFP. It is expected that our approach can be generalized to other algorithms involving the manipulation of components represented using bits. ZFP, which operates on blocks of  $4^d$  values, can encode and truncate data using one of three modes: fixed rate, fixed accuracy, or fixed precision. The fixed rate mode compresses a block to a fixed number of bits, the fixed precision compresses to a variable number of bits while retaining a fixed number of bit planes, and fixed accuracy mode compresses a block with relation to the tolerated maximum error. The goal of this paper is to provide an error analysis for the fixed precision mode, as it is the simplest to represent algebraically. However, as a result of the analysis of the fixed precision mode we are able to develop bounds on the error introduced by the fixed accuracy and fixed rate compression modes.

The remainder of this paper is structured as follows. In the next section, we describe the ZFP compression algorithm. In Section 3, we introduce the notation, definitions, and lemmas that we will use in Section 4 to prove bounds on the error introduced at each stage of the ZFP compression algorithm. In Section 5, we derive the error bounds for the fixed precision mode for the composite compression and decompression action, as well as an error bound for both fixed accuracy and fixed rate modes. Finally, we demonstrate the validity of these results numerically in Section 6.

**2. ZFP Data Compression.** We first provide a brief overview of the current ZFP compression algorithm. Further details of the implementation of ZFP can be found in [14] with modifications described in the software documentation [16]. For clarity purposes, a small example of ZFP is provided in Appendix A.

- Step 1:* The  $d$ -dimensional array is partitioned into arrays of dimension  $4^d$ , called *blocks*. A 2-d example is depicted in Figure 1. If the  $d$ -dimensional array cannot be partitioned exactly into blocks, then the boundary of the  $d$ -dimensional array is padded until an exact partition is possible.
- Step 2:* The floating-point values in each block are converted to a block-floating-point representation using a common exponent for each block [18] and integers in two’s complement format. The block-floating point representation is then shifted and rounded to  $4^d$  signed integers as seen in Figure 2.
- Step 3:* The integers are decorrelated using a custom, high-speed, near orthogonal transform that is similar to the discrete cosine transform. The idea is that continuous fields tend to exhibit autocorrelation which can be viewed as redundant information. The decorrelating transform removes these redundancies via a change in basis resulting in a “sparser” representation with smaller magnitude coefficients. The many leading zeros in the small coefficients offer an opportunity for compression (see Section 4.3 for details.)
- Step 4:* Coefficient magnitude tends to correlate (inversely) with sequency. A 2-d example of total sequency can be seen in Figure 3. Sequency ordering is done to place the coefficients roughly in order of decreasing magnitude, which tends to group ones together and zeros together in each

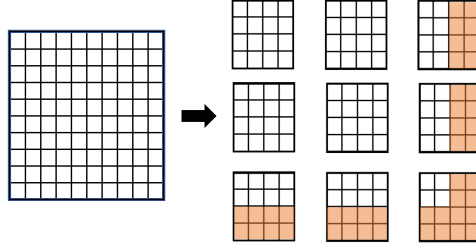


Fig. 1: Deconstruction of a  $10 \times 10$  2-dimensional array into independent  $4 \times 4$  blocks. If the data is not divisible by 4 the data at the boundaries is padded (shown in orange).

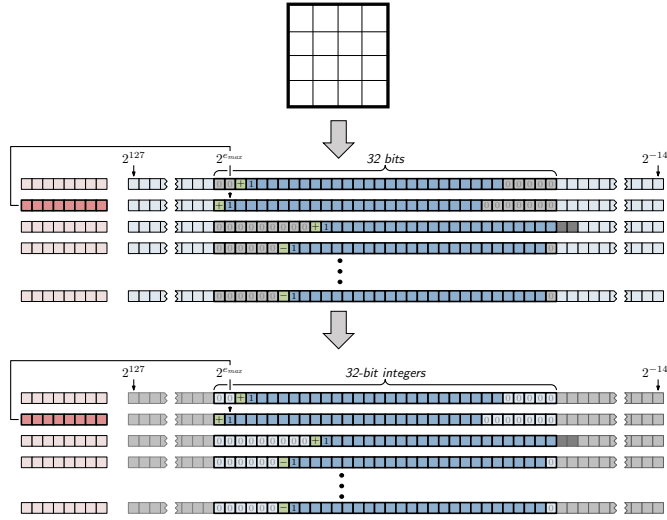


Fig. 2: Floating-point bit representation in single precision converted to a block-floating-point representation and its corresponding signed integers. Note that, depending on the relative disparity of the 16 numbers, some truncation may occur for the numbers of the smallest magnitude.

bit plane. This facilitates compression as often small coefficients tend to share leading zeros.

*Step 5:* The sign bit is typically the left most bit in any traditional binary representation, which does not provide any useful information until the leading one-bit is encountered, i.e., the transition from 0 to 1 (for positive values) or from 1 to 0 (for negative values). However, the first nonzero bit encountered in a negabinary representation immediately informs of the sign and magnitude. For example, if the leftmost one-bit in negabinary is at position  $e$ , then the magnitude of the number is in  $2^e \cdot [1/3, 4/3]$ . If  $e$  is even, then the number is positive; otherwise it is negative. Thus, the two's complement signed integers (the standard integer representation) are converted to their negabinary representation [11]. The negabinary representation also ensures that the error caused by the remaining steps is mostly centered around zero with a slight bias depending on the index of truncated bit-plane.

*Step 6:* The bits that represent the list of  $4^d$  integers are transposed so that they are ordered by bit plane, from most to least significant bit, instead of by coefficient.

*Step 7:* Each bit plane is compressed losslessly using embedded coding, which exploits the property

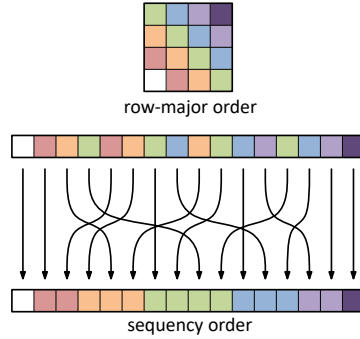


Fig. 3: Total sequency ordering for a 2-dimensional array, which groups the diagonal elements together.

that the transform coefficients tend to have many leading zeros. The idea is to encode groups of zero-bits together using a single bit to indicate that the whole group consists of zeros. As this step is lossless, the encoding details are omitted.

*Step 8:* The embedded coder emits one bit at a time until stopping criterion are satisfied. The exact stopping criteria is dependent on the mode of ZFP compression: either fixed rate, fixed precision, or fixed accuracy.

Most of our discussion and error analysis in Section 4 will focus on Steps 2, 3, and 8 as these steps are likely to introduce additional round-off error during compression and, in some cases, during decompression. Our approach for bounding the round off error introduced by ZFP compression and decompression is to define an operator for each step of the algorithm, compose these operators to form a ZFP compression and a ZFP decompression operator, compute the value returned after compressing and decompressing an arbitrary input, and finally compare this value to the value of the original input. The next section will focus on introducing notation and definitions that will be useful in defining mathematical operators for each step of the ZFP compression algorithm.

**3. Preliminary Notations, Definitions, and Lemmas.** As noted in Section 2, many of the steps of ZFP are defined by direct manipulation of the bits used to represent each component of the input. While we could attempt to define operators that imitate the steps of ZFP over the real vector space, it would be more straightforward to work with the bitwise representation that is manipulated at each step of the ZFP compression algorithm. Hence, in order to define operators for each step of ZFP as actions on the bitwise representation of each component, we construct vector spaces under which the components correspond to binary or negabinary representations of the real numbers. Accordingly, let  $\mathbb{B} = \{0, 1\}$  and define

$$(3.1) \quad \mathcal{C} := \left\{ \{c_i\}_{i=-\infty}^{\infty} : c_i \in \mathbb{B} \text{ for all } i \in \mathbb{Z} \right\}.$$

For  $c \in \mathcal{C}$ , we define the *active bit set of  $c$*  by  $\mathcal{I}(c) := \{i \in \mathbb{Z} : c_i = 1\}$ . Additionally, we define the following operators on  $\mathcal{C}$  that will be used as building blocks for defining each step of ZFP.

**DEFINITION 3.1.** Let  $\mathcal{S} \subseteq \mathbb{Z}$ . The truncation operator,  $t_{\mathcal{S}} : \mathcal{C} \rightarrow \mathcal{C}$ , is defined by

$$t_{\mathcal{S}}(c)_i = \begin{cases} c_i & : i \in \mathcal{S} \\ 0 & : i \notin \mathcal{S} \end{cases}, \quad \text{for all } c \in \mathcal{C} \text{ and all } i \in \mathbb{Z}.$$

Let  $\ell \in \mathbb{Z}$ . The shift operator,  $s_{\ell} : \mathcal{C} \rightarrow \mathcal{C}$ , is defined by

$$s_{\ell}(c)_i = c_{i+\ell}, \quad \text{for all } c \in \mathcal{C} \text{ and all } i \in \mathbb{Z}.$$

Table 1: Notation Table

Symbol	Description	Location
$d$	dimension of the input data	§4.1
$k$	the number of IEEE mantissa bits, including the leading one-bit	§4.2
$q$	the number of consecutive bits used to represent an element in the block-floating point transform	§4.2
$\beta$	number of bit planes kept in Step 8	§4.8
$\mathcal{I}$	active bit set	§3
$\mathcal{B}^n$	infinite binary vector space	§3.1
$\mathcal{B}_k^n$	subset of $\mathcal{B}^n$ with finite active bit set	§3.1
$\mathcal{N}^n$	infinite negabinary vector space	§3.1
$\mathcal{N}_k^n$	subset of $\mathcal{N}^n$ with finite active bit set	§3.1
$\mathbf{0}_{\mathcal{B}}, \mathbf{0}_{\mathcal{N}}$	additive identity in $\mathcal{B}^n$ and $\mathcal{N}^n$ , respectively	§3.1
$\mathbf{1}_{\mathcal{B}}, \mathbf{1}_{\mathcal{N}}$	multiplicative identity in $\mathcal{B}^n$ and $\mathcal{N}^n$ , respectively	§3.1
$\ \cdot\ _{\mathcal{B},p}, \ \cdot\ _{\mathcal{N},p}$	$p$ -norm with respect to $\mathcal{B}^n$ and $\mathcal{N}^n$ , respectively	§3.2
$f_{\mathcal{B}}, f_{\mathcal{B}}^{-1}, f_{\mathcal{N}}, f_{\mathcal{N}}^{-1}$	bijective maps from $\mathcal{B} \rightarrow \mathbb{R}, \mathbb{R} \rightarrow \mathcal{B}, \mathcal{N} \rightarrow \mathbb{R}$ and $\mathbb{R} \rightarrow \mathcal{N}$ , respectively	Eqn. (3.3)
$F_{\mathcal{B}}, F_{\mathcal{B}}^{-1}, F_{\mathcal{N}}, F_{\mathcal{N}}^{-1}$	bijective maps from $\mathcal{B}^n \rightarrow \mathbb{R}^n, \mathbb{R}^n \rightarrow \mathcal{B}^n, \mathcal{N}^n \rightarrow \mathbb{R}^n$ and $\mathbb{R}^n \rightarrow \mathcal{N}^n$ , respectively	§3.1
$\oplus$	bit vector addition	Lma. 3.2
$\odot$	bit vector multiplication	Lma. 3.2
$s_l, S_l$	shift operator on $\mathcal{B}$ and $\mathcal{B}^n$ , respectively	§3.5
$t_{\mathcal{S}_k}, T_{\mathcal{S}_k}$	truncation operator with respect to the set $\mathcal{S}_k$	3.1
$r$	rounding operator for two's complement representation	§4.3
$e_{min}, e_{max}$	min and max exponent of the floating-point representation of the block	Def. 3.5
$\epsilon_m$	constant $\epsilon_m := 2^{1-m}$ , with $m \in \mathbb{N}$	§3.1
$L, L_d$	one and $d$ -dimension forward decorrelating linear transform	Eqn. 4.6
$\tilde{L}, \tilde{L}_d$	floating-point arithmetic approximation of $L$ and $L_d$	§4.3
$L_d^{-1}, \tilde{L}_d^{-1}$	$d$ -dimension backward decorrelating linear transform and the floating-point arithmetic approximation of $L^{-1}$	§4.3
$C_k, \tilde{C}_k$	lossless/lossy operator for Step $k$ of ZFP compression	§4
$D_k, \tilde{D}_k$	lossless/lossy operator for Step $k$ of ZFP decompression	§4

From these definitions, it follows that  $t_{\mathcal{S}}$  is a nonlinear operator and  $s_{\ell}$  is a linear operator. These operators can be extended to operators on  $\mathcal{C}^n$  by defining  $T_{\mathcal{S}} : \mathcal{C}^n \rightarrow \mathcal{C}^n$  and  $S_{\ell} : \mathcal{C}^n \rightarrow \mathcal{C}^n$  by

$$T_{\mathcal{S}}(\mathbf{c}) = \begin{bmatrix} t_{\mathcal{S}}(\mathbf{c}_1) \\ \vdots \\ t_{\mathcal{S}}(\mathbf{c}_n) \end{bmatrix} \quad \text{and} \quad S_{\ell}(\mathbf{c}) = \begin{bmatrix} s_{\ell}(\mathbf{c}_1) \\ \vdots \\ s_{\ell}(\mathbf{c}_n) \end{bmatrix}, \text{ for all } \mathbf{c} \in \mathcal{C}^n.$$

For clarity, note that the components of  $\mathbf{c}$  are each binary sequences as  $\mathbf{c}_i \in \mathcal{C}$ , for  $1 \leq i \leq n$ . Additionally, note that  $S_{\ell}$  is invertible with  $S_{\ell}^{-1} : \mathcal{C}^n \rightarrow \mathcal{C}^n$  given by  $S_{\ell}^{-1} = S_{-\ell}$ .

**3.1. Defining Signed Binary and Negabinary Bit-Vector Spaces.** Let  $x \in \mathbb{R}$  be given. Then there exist  $c, d \in \mathcal{C}$  and  $p \in \mathbb{B}$  such that  $x$  can be represented in signed binary and negabinary as

$$(3.2) \quad \text{Signed Binary: } x = (-1)^p \sum_{i=-\infty}^{\infty} c_i 2^i \quad \text{and} \quad \text{Negabinary: } x = \sum_{i=-\infty}^{\infty} d_i (-2)^i.$$

As such, there exist subsets  $\mathcal{A}$  and  $\mathcal{N}$  of  $\mathcal{C}$  such that, for each  $x \in \mathbb{R}$ , there exist unique elements  $c \in \mathcal{A}$ ,  $p \in \mathbb{B}$ , and  $d \in \mathcal{N}$  such that  $x$  can be represented in the binary and negabinary form in (3.2) using  $c$ ,  $p$ , and  $d$ , respectively. In particular, we choose  $\mathcal{A}$  and  $\mathcal{N}$  such that  $\mathcal{I}(c)$  and  $\mathcal{I}(d)$  are finite whenever possible. This choice is made so that elements can be represented using finitely many nonzero bits. Now define  $0_{\mathcal{C}}, 1_{\mathcal{C}} \in \mathcal{C}$  to be the elements satisfying  $\mathcal{I}(0_{\mathcal{C}}) = \emptyset$  and  $\mathcal{I}(1_{\mathcal{C}}) = \{0\}$ . It follows from our choice of  $\mathcal{A}$  and  $\mathcal{N}$  that  $\{0_{\mathcal{C}}, 1_{\mathcal{C}}\} \subset \mathcal{A} \cap \mathcal{N}$ .

Defining  $\mathcal{B} := \{(p, a) \in \mathbb{B} \times \mathcal{A} : (p, a) \neq (1, 0_{\mathcal{C}})\}$ , we have that, for each  $x \in \mathbb{R}$ , there exists a unique  $b = (p, a) \in \mathcal{B}$  such that  $x = (-1)^p \sum_{i=-\infty}^{\infty} a_i 2^i$ . Additionally, it is clear from our choice of  $\mathcal{N}$  that, for

each  $x \in \mathbb{R}$ , there exists a unique  $d \in \mathcal{N}$  such that  $x = \sum_{i=-\infty}^{\infty} d_i(-2)^i$ . We now define  $f_{\mathcal{B}} : \mathcal{B} \rightarrow \mathbb{R}$  by

$$(3.3) \quad f_{\mathcal{B}}(b) = (-1)^p \sum_{i=-\infty}^{\infty} a_i 2^i, \quad \text{for all } b = (p, a) \in \mathcal{B},$$

and  $f_{\mathcal{N}} : \mathcal{N} \rightarrow \mathbb{R}$  by

$$(3.4) \quad f_{\mathcal{N}}(d) = \sum_{i=-\infty}^{\infty} d_i(-2)^i, \quad \text{for all } d \in \mathcal{N}.$$

By our choice of  $\mathcal{B}$  and  $\mathcal{N}$ ,  $f_{\mathcal{B}}$  and  $f_{\mathcal{N}}$  are bijections and with inverses denoted by  $f_{\mathcal{B}}^{-1} : \mathbb{R} \rightarrow \mathcal{B}$  and  $f_{\mathcal{N}}^{-1} : \mathbb{R} \rightarrow \mathcal{N}$ , respectively. We now define binary operators  $\oplus_{\mathcal{B}} : \mathcal{B} \times \mathcal{B} \rightarrow \mathcal{B}$  and  $\odot_{\mathcal{B}} : \mathcal{B} \times \mathcal{B} \rightarrow \mathcal{B}$  by

$$(3.5) \quad \alpha \oplus_{\mathcal{B}} \beta = f_{\mathcal{B}}^{-1}(f_{\mathcal{B}}(\alpha) + f_{\mathcal{B}}(\beta)) \quad \text{and} \quad \alpha \odot_{\mathcal{B}} \beta = f_{\mathcal{B}}^{-1}(f_{\mathcal{B}}(\alpha) \cdot f_{\mathcal{B}}(\beta))$$

for all  $\alpha, \beta \in \mathcal{B}$ , where  $+$  and  $\cdot$  represent standard addition and multiplication in  $\mathbb{R}$ . Similarly, we can define  $\oplus_{\mathcal{N}} : \mathcal{N} \times \mathcal{N} \rightarrow \mathcal{N}$  and  $\odot_{\mathcal{N}} : \mathcal{N} \times \mathcal{N} \rightarrow \mathcal{N}$  by replacing all  $\mathcal{B}$  with  $\mathcal{N}$  in (3.5). With these definitions in place, we now have the following result.

**LEMMA 3.2.** *( $\mathcal{B}, \oplus_{\mathcal{B}}, \odot_{\mathcal{B}}$ ) and ( $\mathcal{N}, \oplus_{\mathcal{N}}, \odot_{\mathcal{N}}$ ) are fields with additive and multiplicative identities  $0_{\mathcal{B}} := (0, 0_{\mathcal{C}})$  and  $1_{\mathcal{B}} := (0, 1_{\mathcal{C}})$  and  $0_{\mathcal{N}} := 0_{\mathcal{C}}$  and  $1_{\mathcal{N}} := 1_{\mathcal{C}}$ , respectively.*

For the remainder of the discussion, the sign bit will be omitted from elements of  $\mathcal{B}$  by letting  $a$  represent the element  $(0, a) \in \mathcal{B}$  and  $-a$  represent  $(1, a) \in \mathcal{B}$ . Additionally, to simplify the notation in the following sections, we will write  $+$  instead of  $\oplus_{\mathcal{B}}$  or  $\oplus_{\mathcal{N}}$  where the operation should be clear from the context in which it is used.

Note that  $f_{\mathcal{B}}$  and  $f_{\mathcal{N}}$  can be generalized to vector-valued functions by defining  $F_{\mathcal{B}} : \mathcal{B}^n \rightarrow \mathbb{R}^n$  and  $F_{\mathcal{N}} : \mathcal{N}^n \rightarrow \mathbb{R}^n$  as  $F_{\mathcal{B}}(\mathbf{a}) = [f_{\mathcal{B}}(\mathbf{a}_1), \dots, f_{\mathcal{B}}(\mathbf{a}_n)]^t$  and  $F_{\mathcal{N}}(\mathbf{d}) = [f_{\mathcal{N}}(\mathbf{d}_1), \dots, f_{\mathcal{N}}(\mathbf{d}_n)]^t$ , where  $\mathbf{a} \in \mathcal{B}^n$  and  $\mathbf{d} \in \mathcal{N}^n$ , respectively. By definition,  $F_{\mathcal{B}}$  and  $F_{\mathcal{N}}$  are invertible with inverses  $F_{\mathcal{B}}^{-1}$  and  $F_{\mathcal{N}}^{-1}$  defined by applying  $f_{\mathcal{B}}^{-1}$  and  $f_{\mathcal{N}}^{-1}$  componentwise, respectively. We will let  $\mathbf{0}_{\mathcal{B}}$  and  $\mathbf{0}_{\mathcal{N}}$  denote the additive identity in  $\mathcal{B}^n$  and  $\mathcal{N}^n$ , respectively, and  $I_{\mathcal{B}} : \mathcal{B}^n \rightarrow \mathcal{B}^n$  and  $I_{\mathcal{N}} : \mathcal{N}^n \rightarrow \mathcal{N}^n$  denote the identity map on  $\mathcal{B}^n$  and  $\mathcal{N}^n$ , respectively.

To imitate floating-point representations we define the following subsets of  $\mathcal{B}$  and  $\mathcal{N}$ . Given  $k \in \mathbb{N}$ ,

$$\mathcal{B}_k = \{(p, a) \in \mathcal{B} : \mathcal{I}(a) \subseteq \{i, i+1, \dots, i+k-1\} \text{ for some } i \in \mathbb{Z}\}$$

and

$$\mathcal{N}_k = \{d \in \mathcal{N} : \mathcal{I}(d) \subseteq \{i, i+1, \dots, i+k-1\} \text{ for some } i \in \mathbb{Z}\}.$$

Here,  $k$  represents the maximum number of nonzero bits allotted for each representation. For example, in  $\mathcal{B}_k$ ,  $k$  represents the number of bits allotted for the mantissa and  $i$  indicates the exponent in IEEE. It should be noted that  $\mathcal{B}_k$  and  $\mathcal{N}_k$  are subsets but *not* subspaces of  $\mathcal{B}$  and  $\mathcal{N}$ , respectively, as they do not satisfy the property of closure under  $\oplus$  and  $\odot$ . As such, the analysis will take place in  $\mathcal{B}$ ,  $\mathcal{N}$ , or  $\mathbb{R}$  with the use of the truncation operator,  $T_{\mathcal{S}}$ , to imitate working with finite precision elements.

**3.2. Meaningful Norms on  $\mathcal{B}^n$  and  $\mathcal{N}^n$ .** From Lemma 3.2, it follows that  $\mathcal{B}^n$  is a vector space under  $+$ . Let  $\|\cdot\|_p$  be the standard  $p$ -norm on  $\mathbb{R}^n$ . Accordingly, we define  $\|\cdot\|_{\mathcal{B},p} : \mathcal{B}^n \rightarrow [0, \infty)$  by

$$(3.6) \quad \|\mathbf{a}\|_{\mathcal{B},p} = \begin{cases} (\sum_{i=1}^n |f_{\mathcal{B}}(\mathbf{a}_i)|^p)^{1/p} & : 1 \leq p < \infty \\ \max_{1 \leq i \leq n} |f_{\mathcal{B}}(\mathbf{a}_i)| & : p = \infty \end{cases}$$

The following result is an immediate consequence from the definition of  $\|\cdot\|_{\mathcal{B},p}$ .

LEMMA 3.3. For all  $\mathbf{a} \in \mathcal{B}^n$ ,  $\mathbf{x} \in \mathbb{R}^n$ , and  $1 \leq p \leq \infty$ ,  $\|\cdot\|_{\mathcal{B},p}$  is a norm satisfying

$$\|F_{\mathcal{B}}(\mathbf{a})\|_p = \|\mathbf{a}\|_{\mathcal{B},p} \quad \text{and} \quad \|\mathbf{x}\|_p = \|F_{\mathcal{B}}^{-1}(\mathbf{x})\|_{\mathcal{B},p}.$$

For any  $1 \leq p \leq \infty$ , we now have that  $\mathcal{B}^n$  is a normed vector space with norm  $\|\cdot\|_{\mathcal{B},p}$ . Additionally, we can define a norm for operators defined on  $\mathcal{B}^n$ .

DEFINITION 3.4. Let  $m, n \in \mathbb{N}$  and  $1 \leq p \leq \infty$ . The induced  $p$ -norm on  $\Phi : \mathcal{B}^n \rightarrow \mathcal{B}^m$  is given by

$$\|\Phi\|_{\mathcal{B},p} = \sup \left\{ \frac{\|\Phi(\mathbf{a})\|_{\mathcal{B},p}}{\|\mathbf{a}\|_{\mathcal{B},p}} : \mathbf{a} \in \mathcal{B}^n, \mathbf{a} \neq \mathbf{0}_{\mathcal{B}} \right\}.$$

As an immediate consequence of this definition,  $\|\Phi(\mathbf{a})\|_{\mathcal{B},p} \leq \|\Phi\|_{\mathcal{B},p} \|\mathbf{a}\|_{\mathcal{B},p}$  holds for all  $\mathbf{a} \in \mathcal{B}^n \setminus \mathbf{0}_{\mathcal{B}}$ . In a similar manner, given  $1 \leq p \leq \infty$  we can define the norm  $\|\cdot\|_{\mathcal{N},p}$  over  $\mathcal{N}$  satisfying a result analogous to Lemma 3.3 by replacing every  $\mathcal{B}$  by  $\mathcal{N}$  in (3.6) and Definition 3.4.

**3.3. Two's Complement.** From the end of Step 2 through the beginning of Step 5, the ZFP implementation stores the integer components of each block using a normalized fixed-point, two's complement binary integer representation. For  $z \in \mathbb{Z}$ , the two's complement representation is of the form

$$\text{Two's Complement:} \quad z = -t_{N-1}2^{N-1} + \sum_{i=0}^{N-2} t_i 2^i,$$

for some  $N \in \mathbb{N}$  and some  $t \in \mathcal{C}$ . Typically, the value of  $N$  is chosen beforehand to be the number of bits allotted for storing each integer. Unfortunately, this aspect of the two's complement representation does not lend itself to a construction of a vector space, unlike  $\mathcal{B}^n$  and  $\mathcal{N}^n$  constructed in Section 3.1. Thus, instead of working explicitly in two's complement, we will take care when defining operators for Steps 2 through 5 in  $\mathcal{B}^n$  to ensure they mimic the behavior of the two's complement representation used in ZFP.

**3.4. Truncation Operator on  $\mathcal{B}^n$  and  $\mathcal{N}^n$ .** In this section, we consider some properties of the truncation operator,  $T_S(\cdot)$ , over the normed vector spaces  $\mathcal{B}^n$  and  $\mathcal{N}^n$ . The usefulness of these definitions and results will be evident during the analysis of the ZFP compression algorithm in Section 5.

DEFINITION 3.5. Let  $\mathbf{x} \in \mathbb{R}^n$ . The maximum exponent of  $\mathbf{x}$  with respect to  $\mathcal{B}$  is

$$(3.7) \quad e_{max,\mathcal{B}}(\mathbf{x}) = \max_{1 \leq i \leq n} \max_j \{j \in \mathcal{I}(f_{\mathcal{B}}^{-1}(\mathbf{x}_i))\},$$

and minimum exponent of  $\mathbf{x}$  with respect to  $\mathcal{B}$  is

$$(3.8) \quad e_{min,\mathcal{B}}(\mathbf{x}) = \min_{1 \leq i \leq n} \min_j \{j \in \mathcal{I}(f_{\mathcal{B}}^{-1}(\mathbf{x}_i))\},$$

provided that the minimum exists. Similarly, we define the maximum and minimum exponent of  $\mathbf{x}$  with respect to  $\mathcal{N}$  by replacing  $\mathcal{B}$  with  $\mathcal{N}$  in (3.7) and (3.8).

When it is clear from context which space,  $\mathcal{B}$  or  $\mathcal{N}$ , the vector  $\mathbf{x}$  is in, we will simply write  $e_{max}$  or  $e_{min}$ . The next result provides a relation between elements of  $\mathcal{B}$  and  $\mathcal{N}$  and  $e_{max}$ .

LEMMA 3.6. For  $\mathbf{a} \in \mathcal{B}^n$ ,  $\mathbf{d} \in \mathcal{N}^n$ : (i)  $\|\mathbf{a}\|_{\mathcal{B},\infty} \geq 2^{e_{max,\mathcal{B}}(F_{\mathcal{B}}(\mathbf{a}))}$  (ii)  $\|\mathbf{d}\|_{\mathcal{N},\infty} \geq \frac{1}{3}2^{e_{max,\mathcal{N}}(F_{\mathcal{N}}(\mathbf{d}))}$ .

*Proof.* (i) follows immediately from the definition of  $e_{max,\mathcal{B}}(\mathbf{x})$ . Next, for  $z \in \mathbb{Z}$  even we define  $\mathcal{J}(z) = \{2j \in \mathbb{Z} : 2j \leq z\}$  and for  $z \in \mathbb{Z}$  odd we define  $\mathcal{J}(z) = \{2j + 1 \in \mathbb{Z} : 2j + 1 \leq z\}$ . Letting  $e = e_{max,\mathcal{N}}(\mathbf{x})$ , (ii) follows from observing

$$\|\mathbf{d}\|_{\mathcal{N},\infty} \geq \left| (-2)^e - \sum_{i \in \mathcal{J}(e-1)} (-2)^i \right| = 2^e - \frac{2}{3}2^e = \frac{1}{3}2^{e_{max,\mathcal{N}}(F_{\mathcal{N}}(\mathbf{d}))}. \quad \square$$

We now provide a result establishing the relationship between  $\mathbf{a}$  and  $T_{\mathcal{S}}(\mathbf{a})$  given  $\mathbf{a} \in \mathcal{B}^n$  or  $\mathbf{a} \in \mathcal{N}^n$ . First, note that for certain choices of  $m \in \mathbb{Z}$  the constant term  $2^{1-m}$  will regularly occur in error bounds established throughout this paper. Hence, we will let  $\epsilon_m := 2^{1-m}$  for any  $m \in \mathbb{Z}$ . For example, machine epsilon [9] is defined as  $\epsilon_k = 2^{1-k}$  for precision  $k$ .

LEMMA 3.7. *Suppose  $p, q \in \mathbb{Z}$  and let  $\mathcal{S} = \{i \in \mathbb{Z} : i > p - q\}$ . If  $\mathbf{a} \in \mathcal{B}^n$  and  $\mathbf{d} \in \mathcal{N}^n$  then*

- (i)  $\mathbf{a} = T_{\mathcal{S}}(\mathbf{a}) + \Delta\mathbf{a}$ , for some  $\Delta\mathbf{a} \in \mathcal{B}^n$  satisfying  $\|\Delta\mathbf{a}\|_{\mathcal{B},\infty} \leq \epsilon_q 2^p$ .
- (ii)  $\mathbf{d} = T_{\mathcal{S}}(\mathbf{d}) + \Delta\mathbf{d}$ , for some  $\Delta\mathbf{d} \in \mathcal{N}^n$  satisfying  $\|\Delta\mathbf{d}\|_{\mathcal{N},\infty} \leq \frac{2}{3}\epsilon_q 2^p$ .

*Proof.* Let  $1 \leq m \leq n$ . Observing

$$|f_{\mathcal{B}}(\Delta\mathbf{a}_m)| = |f_{\mathcal{B}}(\mathbf{a}_m - T_{\mathcal{S}}(\mathbf{a})_m)| = \sum_{i \in \mathcal{I}(\mathbf{a}_m \ominus T_{\mathcal{S}}(\mathbf{a})_m)} 2^i \leq \sum_{i=-\infty}^{p-q} 2^i = 2^{p-q+1}$$

concludes the proof of (i). Next, for  $z \in \mathbb{Z}$  even we define  $\mathcal{J}(z) = \{2j \in \mathbb{Z} : 2j \leq z\}$  and for  $z \in \mathbb{Z}$  odd we define  $\mathcal{J}(z) = \{2j + 1 \in \mathbb{Z} : 2j + 1 \leq z\}$ . Then (ii) follows by observing that

$$|f_{\mathcal{N}}(\Delta\mathbf{d}_m)| = |f_{\mathcal{N}}(\mathbf{d}_m - T_{\mathcal{S}}(\mathbf{d})_m)| = \left| \sum_{i \in \mathcal{I}(\mathbf{a}_m \ominus T_{\mathcal{S}}(\mathbf{a})_m)} (-2)^i \right| \leq \left| \sum_{i \in \mathcal{J}(p-q)} (-2)^i \right| = \frac{2}{3} 2^{p-q+1}. \quad \square$$

Hence, if  $\mathcal{S} = \{i \in \mathbb{Z} : i > e_{\max}(F_{\mathcal{B}}(\mathbf{a})) - q\}$  then the additional round-off error incurred by the truncation operator is dependent on  $q$  and the magnitude of the input. Using Lemma 3.7, we now observe that the component-wise relative error introduced by the truncation operator is bounded by

$$(3.9) \quad \max_{m, f_{\mathcal{B}}(\mathbf{a}_m) \neq 0} f_{\mathcal{B}} \left( \left| \frac{\mathbf{a}_m - T_{\mathcal{S}}(\mathbf{a}_m)}{\mathbf{a}_m} \right| \right) \leq \frac{\|\Delta\mathbf{a}\|_{\mathcal{B},\infty}}{\min_{m, f_{\mathcal{B}}(\mathbf{a}_m) \neq 0} f_{\mathcal{B}}(|\mathbf{a}_m|)} = \epsilon_q 2^{e_{\max}(F_{\mathcal{B}}(\mathbf{a})) - e_{\min}(F_{\mathcal{B}}(\mathbf{a}))},$$

for  $\mathbf{a} \in \mathcal{B}^n$  with  $F_{\mathcal{B}}(\mathbf{a}) \neq \mathbf{0}$ . So the component-wise error relative to the input is dependent on  $q$  and the exponent range, i.e.,  $\rho = e_{\max}(F_{\mathcal{B}}(\mathbf{a})) - e_{\min}(F_{\mathcal{B}}(\mathbf{a}))$ . In [14], it was noted that in many real-world examples, the exponent range was reasonable ( $\rho \leq 8$ ). Thus, depending on  $\rho$ ,  $q$  could be chosen to ensure the component-wise error relative to the input remains smaller than machine epsilon.

**3.5. Shift Operator on  $\mathcal{B}^n$ .** We now wish to determine what can be said about the norm of the shift operator defined on  $\mathcal{B}^n$ . For  $a \in \mathcal{B}$  and  $\ell \in \mathbb{Z}$ , observe that

$$|f_{\mathcal{B}}(s_{\ell}(a))| = \left| \sum_{i \in \mathcal{I}(a)} 2^{i-\ell} \right| = 2^{-\ell} \left| \sum_{i \in \mathcal{I}(a)} 2^i \right| = 2^{-\ell} |f_{\mathcal{B}}(a)|.$$

This observation, together with the definition of  $\|\cdot\|_{\mathcal{B},p}$ , yields the following result.

LEMMA 3.8. *Suppose  $\ell \in \mathbb{Z}$  and  $1 \leq p \leq \infty$ . Then  $\|S_{\ell}\|_{\mathcal{B},p} = 2^{-\ell}$  and  $\|S_{\ell}^{-1}\|_{\mathcal{B},p} = 2^{\ell}$ .*

To summarize, we have constructed the normed vector spaces  $\mathcal{B}^n$  and  $\mathcal{N}^n$  and bijective maps between  $\mathcal{B}^n$  and  $\mathbb{R}^n$  and  $\mathcal{N}^n$  and  $\mathbb{R}^n$ . We can represent floating-point or fixed-point representations by applying the truncation operator  $T_{\mathcal{S}}(\cdot)$  on elements of  $\mathcal{B}^n$  or  $\mathcal{N}^n$ , and multiplication by powers of two in  $\mathbb{R}^n$  is equivalent to applying shift operator,  $S_{\ell}$ , to elements in  $\mathcal{B}^n$ . We now have the tools to define operators for each step of the ZFP compression algorithm, as described in Section 2.

**4. Error Analysis of Individual Steps of the ZFP Compression Algorithm.** The goals of this section are to define operators for each step of the ZFP compression algorithm and to determine the error resulting from each step. For each step of ZFP, we define an operator that carries out the implemented version of ZFP compression and decompression as well as a lossless version. The lossless



version of each operator will be useful in determining the error introduced at each step of the algorithm. Decompression for steps corresponding to invertible compression steps are merely the inverse operators of the compression step. Since ZFP compression is lossy in nature, some of the steps implemented in the compression phase are not invertible. For such steps, the corresponding decompression step is defined by an injective map that restores only the information that has not been lost to the correct format for the next step of decompression. For the sake of brevity, any step of the algorithm that does not affect the error analysis will not be considered in much depth.

**4.1. Partition  $d$ -dimensional array into blocks of  $4^d$  values.** In Step 1, the  $d$ -dimensional array is partitioned into blocks of size  $4^d$ . Since Steps 2 through 8 are then applied to each  $4^d$  block individually, it is not necessary to consider Step 1 in the error analysis. Accordingly, we do not define any operators for this step.

**4.2. Block-Floating-Point Transform.** Suppose that  $\mathbf{x} \in \mathbb{R}^{4^d}$  such that  $F_{\mathcal{B}}^{-1}(\mathbf{x}) \in \mathcal{B}_k^{4^d}$  for some precision  $k$  (i.e., every element in  $\mathbf{x}$  can be represented with at most  $k$ -consecutive bits). For frequently used IEEE floating-point types,  $k \in \{24, 53\}$ . This assumption on  $\mathbf{x}$  implies that we are working with a floating point representation of a real number. To perform Step 2, we first convert each component in  $\mathbf{x}$  to its corresponding representation in  $\mathcal{B}$ . Each element is then shifted to the left by a deterministic number of bits and truncated. As a by-product of type-casting to an integer, in the implementation of ZFP, each value is rounded down to zero. Applying the shift operator followed by the truncation operator, as outlined above, results in the same outcome.

The operator in Step 2 is dependent on the fixed set  $\mathcal{S} := \{i \in \mathbb{Z} : i \geq 0\}$  and the value  $q \in \mathbb{N}$ , where  $q$  denotes the maximum number of nonzero consecutive bits (precision) that can be used for the representation of each component of the input. ZFP requires each value to have one bit as a safe-guard against overflow, which occurs when the calculation produces a result that exceeds the capacity of the finite bit representation. In the current ZFP implementation, if the input values are IEEE single or double precision,  $q \in \{30, 62\}$  in  $\mathcal{B}$ , since one bit is used to represent the sign bit and another to represent the overflow guard bit. Step 2 is defined by the map  $\tilde{C}_2 : \mathbb{R}^{4^d} \rightarrow \mathcal{B}^{4^d}$  where

$$*\tilde{C}_2(\mathbf{x}) := T_{\mathcal{S}} S_{\ell} F_{\mathcal{B}}^{-1}(\mathbf{x}), \text{ for all } \mathbf{x} \in \mathbb{R}^{4^d},$$

where  $\ell = e_{\max}(F_{\mathcal{B}}^{-1}(\mathbf{x})) - q + 1$ . We define the lossless operator,  $C_2$ , by removing all noninvertible maps from  $\tilde{C}_2$ . Hence,

$$C_2(\mathbf{x}) := S_{\ell} F_{\mathcal{B}}^{-1}(\mathbf{x}).$$

The decompression operator for Step 2 converts the block-floating point back to its original floating-point representation that is representable in  $\mathcal{B}_k$  for  $k \in \mathbb{N}$ . In IEEE, the  $q \in \{30, 62\}$  consecutive bits must be converted back to  $k \in \{24, 53\}$  with its respective exponent information. This conversion can be seen as a typical floating-point round off error. The lossy decompression operator for Step 2 is then defined by undoing the shift performed in  $\tilde{C}_2$  and converting each component back to a floating point representation. Hence,  $\tilde{D}_2 : \mathcal{B}^{4^d} \rightarrow \mathbb{R}^{4^d}$  is defined by

$$\tilde{D}_2(\mathbf{a}) := F_{\mathcal{B}} S_{-\ell} fl_k(\mathbf{a}), \text{ for all } \mathbf{a} \in \mathcal{B}^{4^d},$$

where  $fl_k(\mathbf{a})_i = t_{\mathcal{R}_{ik}}(\mathbf{a}_i)$  with  $\mathcal{R}_{ik} = \{j \in \mathbb{Z} : j > e_{\max, \mathcal{B}}(\mathbf{a}_i) - k\}$ , for all  $1 \leq i \leq 4^d$ . Note that the  $fl_k$  operator converts each component of  $\mathbf{a}$  to a floating point representation with  $k$  mantissa bits in a bit vector format. The lossless decompression operator is then defined as  $D_2 : \mathcal{B}^{4^d} \rightarrow \mathbb{R}^{4^d}$  with  $D_2(\mathbf{a}) := F_{\mathcal{B}} S_{-\ell}(\mathbf{a})$ , for all  $\mathbf{a} \in \mathcal{B}^{4^d}$ . We conclude our discussion of this step by presenting a result that will be useful during the error analysis in Section 5.

**PROPOSITION 4.1.** *Suppose  $\mathbf{x} \in \mathbb{R}^{4^d}$  and  $\mathbf{a} \in \mathcal{B}^{4^d}$ , such that  $e_{\max, \mathcal{B}}(F_{\mathcal{B}}(\mathbf{a})) \geq q - 1$ .*

- (i) Then  $\|\tilde{C}_2\mathbf{x} - C_2\mathbf{x}\|_\infty \leq 2^{-\ell}\epsilon_q\|\mathbf{x}\|_\infty$ .  
(ii) Then  $\|\tilde{D}_2\mathbf{a} - D_2\mathbf{a}\|_\infty \leq 2^\ell\epsilon_k\|\mathbf{a}\|_\infty$ .

*Proof.* For (i), observe that

$$(4.1) \quad \|\tilde{C}_2\mathbf{x} - C_2\mathbf{x}\|_{\mathcal{B},\infty} = \|T_S S_\ell F_{\mathcal{B}}^{-1}(\mathbf{x}) - S_\ell F_{\mathcal{B}}^{-1}(\mathbf{x})\|_{\mathcal{B},\infty} \leq \epsilon_q \|S_\ell F_{\mathcal{B}}^{-1}(\mathbf{x})\|_{\mathcal{B},\infty},$$

$$(4.2) \quad \leq 2^{-\ell}\epsilon_q\|\mathbf{x}\|_\infty,$$

where the inequality in (4.1) follows from Lemma 3.7 (i) and Lemma 3.6 (i). From Lemma 3.8, we have that  $\|S_\ell\|_{\mathcal{B},\infty} = 2^{-\ell}$ , and from Lemma 3.3, we have  $\|F_{\mathcal{B}}^{-1}(\mathbf{x})\|_{\mathcal{B},\infty} = \|\mathbf{x}\|_\infty$ . These together yield the inequality in (4.2). Next, (ii) follows from an argument similar to the proof of (i) by observing that  $\|\tilde{D}_2\mathbf{a} - D_2\mathbf{a}\|_\infty = \|F_{\mathcal{B}} S_{-\ell} fl_k(\mathbf{a}) - F_{\mathcal{B}} S_{-\ell}(\mathbf{a})\|_\infty \leq 2^\ell \|fl_k(\mathbf{a}) - \mathbf{a}\|_{\mathcal{B},\infty} \leq 2^\ell\epsilon_k\|\mathbf{a}\|_{\mathcal{B},\infty}$ .  $\square$

**4.3. Decorrelating Linear Transform.** In Step 3, the output from Step 2 is acted on by a linear transformation,  $L$ .  $L$  is a near-orthogonal transform that is similar to the discrete cosine transform, both of which possess the energy compaction property [19], i.e., most of the signal energy is confined to the first, lowest-frequency transform coefficients. In  $d$ -dimensions, the transform operator can be applied to each dimension separately, and the operator can be represented as a Kronecker product. For  $A \in \mathbb{R}^{n_1, m_1}$  and  $B \in \mathbb{R}^{n_2, m_2}$ , the Kronecker product is defined as

$$A \otimes B = \begin{bmatrix} a_{1,1}B & a_{1,2}B & \cdots & a_{1,m_1}B \\ \vdots & \ddots & & \vdots \\ a_{n_1,1}B & a_{n_1,2}B & \cdots & a_{n_1,m_1}B \end{bmatrix}.$$

Then, the total forward transform operator used in of ZFP is defined as

$$L_d = \underbrace{L \otimes L \otimes \cdots \otimes L}_{(d-1)\text{-products}}$$

where  $L \in \mathbb{R}^{4 \times 4}$  is defined by

$$(4.3) \quad L = \frac{1}{16} \begin{bmatrix} 4 & 4 & 4 & 4 \\ 5 & 1 & -1 & -5 \\ -4 & 4 & 4 & -4 \\ -2 & 6 & -6 & 2 \end{bmatrix} \quad \text{and} \quad L^{-1} = \frac{1}{4} \begin{bmatrix} 4 & 6 & -4 & -1 \\ 4 & 2 & 4 & 5 \\ 4 & -2 & 4 & -5 \\ 4 & -6 & -4 & 1 \end{bmatrix}.$$

Note that  $\|L\|_\infty = 1$  and  $\|L^{-1}\|_\infty = 15/4$ .

First, we define the lossless compression operator for Step 3 by  $C_3 : \mathcal{B}^{4^d} \rightarrow \mathcal{B}^{4^d}$ , where

$$(4.4) \quad C_3(\mathbf{a}) = F_{\mathcal{B}}^{-1} L_d F_{\mathcal{B}}(\mathbf{a}), \text{ for all } \mathbf{a} \in \mathcal{B}^{4^d}.$$

In order to define the lossy operator used in the implementation, it is necessary to account for the finite bit constraint on a machine. Based on Step 2 of ZFP compression, the components provided as the input for Step 3 represent integers. Hence, for some  $q \in \mathbb{N}$ , it follows that the input for Step 3 is an element of  $\mathcal{B}_q^{4^d}$ . Here,  $q$  represents the number of bits available for storing each component. As  $\mathcal{B}_q$  is not closed under addition and multiplication, given  $a, b \in \mathcal{B}_q$ , addition or multiplication of  $a$  and  $b$  may not result in an element of  $\mathcal{B}_q$  and must be rounded. This circumstance is referred to as round-off; error that occurs when the calculation produces a result that exceeds the capacity of the finite bit representation. Since the transformation could result in round-off, the operator used in the implementation of the algorithm will be defined as

$$(4.5) \quad \tilde{C}_3 = F_{\mathcal{B}}^{-1} \tilde{L}_d F_{\mathcal{B}}(\mathbf{a}), \text{ for all } \mathbf{a} \in \mathcal{B}^{4^d},$$

where  $\tilde{L}_d$  is an operator such that  $\tilde{L}_d F_{\mathcal{B}}(\mathbf{a}) \in \mathcal{B}_q^{4^d}$ , for all  $\mathbf{a} \in \mathcal{B}^{4^d}$ .

As the linear transform operator,  $L$ , is invertible, the lossless decompression operator  $D_3 : \mathcal{B}^{4^d} \rightarrow \mathcal{B}^{4^d}$  is defined as

$$D_3(\mathbf{a}) = F_{\mathcal{B}}^{-1} L_d^{-1} F_{\mathcal{B}}(\mathbf{a}), \text{ for all } \mathbf{a} \in \mathcal{B}^{4^d}.$$

Again, since the operation  $L_d^{-1}$  may result in round-off, the operator used in the implementation is defined as

$$\tilde{D}_3(\mathbf{a}) = F_{\mathcal{B}}^{-1} \tilde{L}_d^{-1} F_{\mathcal{B}}(\mathbf{a}), \text{ for all } \mathbf{a} \in \mathcal{B}^{4^d},$$

where  $\tilde{L}_d^{-1}$  is an approximation of  $L_d^{-1}$ .

From [9] (Equation (3.12)), the forward error bound of the floating-point representation of a matrix-vector product,  $L_d \mathbf{x} \in \mathbb{R}^{4^d}$ , is

$$(4.6) \quad \left\| L_d \mathbf{x} - \tilde{L}_d \mathbf{x} \right\|_p \leq \gamma \|L_d\|_p \|\mathbf{x}\|_p,$$

where  $\gamma = 4^d \epsilon_m / (1 - 4^d \epsilon_m)$  and  $\epsilon_m = 2^{1-m}$  represents machine epsilon with precision  $m$ . From [12], we have that  $\|L_d\|_p \leq \|L\|_p^d$ , for  $1 \leq p \leq \infty$ . Hence, (4.6) yields

$$(4.7) \quad \left\| L_d \mathbf{x} - \tilde{L}_d \mathbf{x} \right\|_p \leq \gamma \|L\|_p^d \|\mathbf{x}\|_p.$$

Note that  $\tilde{L}_d^{-1}$  satisfies a forward error bound analogous to (4.7). The forward error bound represented in (4.7) is the worst possible error that can occur for an arbitrary linear transform. As ZFP uses particular transformations, we aim to establish bounds specific to the transformations  $L_d$  and  $L_d^{-1}$ . Accordingly, we note that the action of  $L$  and  $L^{-1}$  can be written in a very efficient C implementation. The action of  $L$  and  $L^{-1}$  on  $\mathbf{a} = [\mathbf{a}_1, \mathbf{a}_2, \mathbf{a}_3, \mathbf{a}_4]^T \in \mathcal{B}^4$  under this implementation is outlined in Table 2.

$L$			$L^{-1}$		
$\mathbf{a}_1 \leftarrow \mathbf{a}_1 + \mathbf{a}_4$	$\mathbf{a}_1 \leftarrow s_1(\mathbf{a}_1)$	$\mathbf{a}_4 \leftarrow \mathbf{a}_4 - \mathbf{a}_1$	$\mathbf{a}_2 \leftarrow \mathbf{a}_2 + s_1(\mathbf{a}_4)$	$\mathbf{a}_4 \leftarrow \mathbf{a}_4 - s_1(\mathbf{a}_2)$	
$\mathbf{a}_3 \leftarrow \mathbf{a}_3 + \mathbf{a}_2$	$\mathbf{a}_3 \leftarrow s_1(\mathbf{a}_3)$	$\mathbf{a}_2 \leftarrow \mathbf{a}_2 - \mathbf{a}_3$	$\mathbf{a}_2 \leftarrow \mathbf{a}_2 + \mathbf{a}_4$	$\mathbf{a}_4 \leftarrow s_{-1}(\mathbf{a}_4)$	$\mathbf{a}_4 \leftarrow \mathbf{a}_4 - \mathbf{a}_2$
$\mathbf{a}_1 \leftarrow \mathbf{a}_1 + \mathbf{a}_3$	$\mathbf{a}_1 \leftarrow s_1(\mathbf{a}_1)$	$\mathbf{a}_3 \leftarrow \mathbf{a}_3 - \mathbf{a}_1$	$\mathbf{a}_3 \leftarrow \mathbf{a}_3 + \mathbf{a}_1$	$\mathbf{a}_1 \leftarrow s_{-1}(\mathbf{a}_1)$	$\mathbf{a}_1 \leftarrow \mathbf{a}_1 - \mathbf{a}_3$
$\mathbf{a}_4 \leftarrow \mathbf{a}_4 + \mathbf{a}_2$	$\mathbf{a}_4 \leftarrow s_1(\mathbf{a}_4)$	$\mathbf{a}_2 \leftarrow \mathbf{a}_2 - \mathbf{a}_4$	$\mathbf{a}_2 \leftarrow \mathbf{a}_2 + \mathbf{a}_3$	$\mathbf{a}_3 \leftarrow s_{-1}(\mathbf{a}_3)$	$\mathbf{a}_3 \leftarrow \mathbf{a}_3 - \mathbf{a}_2$
$\mathbf{a}_4 \leftarrow \mathbf{a}_4 + s_1(\mathbf{a}_2)$	$\mathbf{a}_2 \leftarrow \mathbf{a}_2 - s_1(\mathbf{a}_4)$		$\mathbf{a}_4 \leftarrow \mathbf{a}_4 + \mathbf{a}_1$	$\mathbf{a}_1 \leftarrow s_{-1}(\mathbf{a}_1)$	$\mathbf{a}_1 \leftarrow \mathbf{a}_1 - \mathbf{a}_4$

Table 2: Bit arithmetic steps for ZFP's forward (left) and backward (right) transform (read from left to right).

This implementation is straightforward and efficient as it only requires bit addition/subtraction and division/multiplication by two. In ZFP, the bit vectors are padded so that any overflow that may occur is represented (i.e., for each component in the block one extra bit is allotted to ensure that, if a calculation results in a value greater than what can be represented in  $q$  bits, then the value is not approximated). Thus, for the following analysis, it suffices to calculate the error due to round-off. Additionally, as the components of the input for Step 3 represent signed integers, round-off can only occur during division by two (i.e., one bit shift to the right using  $s_1(\cdot)$ ).

As noted in Section 3.3, care must be taken in Step 3, since the implementation of ZFP uses a two's complement representation of each integer. For our error analysis, the main concern is that rounding to an integer in two's complement after a right bit shift always results in rounding towards negative infinity. However, under the representation defined in  $\mathcal{B}$ , this same sequence of operations results in

rounding towards zero. So, in order to mimic the implementation, we define the operator  $r : \mathcal{B} \rightarrow \mathcal{B}$  by

$$r(a) := \begin{cases} t_{\mathcal{S}}s_1(a) & : f_{\mathcal{B}}(a) \geq 0, \\ t_{\mathcal{S}}s_1(a - 1_{\mathcal{B}}) & : f_{\mathcal{B}}(a) < 0, \end{cases}$$

for all  $a \in \mathcal{B}$ . Since  $s_1(\cdot)$  performs a single right bit shift and  $t_{\mathcal{S}}(\cdot)$ , where  $\mathcal{S} = \{i \in \mathbb{Z} : i \geq 0\}$ , rounds the value towards zero,  $r(\cdot)$  will always round the right bit shift toward negative infinity. The following lemma considers the error of  $r(\cdot)$  when compared to  $s_1(\cdot)$ .

LEMMA 4.2. *Suppose  $\mathcal{S} = \{i \in \mathbb{Z} : i \geq 0\}$  and  $p \in \mathbb{Z}$ . If  $a = f_{\mathcal{B}}^{-1}(p)$ , then  $\|r(a) - s_1(a)\|_{\mathcal{B},\infty} \leq \frac{1}{2}$ .*

*Proof.* As  $p \in \mathbb{Z}$  and  $a = f_{\mathcal{B}}^{-1}(p)$ , we have that  $\mathcal{I}(a) \subseteq \{i \in \mathbb{Z} : i \geq 0\}$ . Now suppose  $p \geq 0$ . Then

$$\mathcal{I}(r(a)) = \mathcal{I}(t_{\mathcal{S}}s_1(a)) = \mathcal{I}(s_1(a)) \setminus \{-1\}.$$

Hence,  $\|r(a) - s_1(a)\|_{\mathcal{B},\infty} \leq \frac{1}{2}$ .

On the other hand, suppose  $p < 0$ . If  $p$  is even, then  $p = 2k$  for some  $k \in \mathbb{Z}$ , and  $f_{\mathcal{B}}(r(a)) = f_{\mathcal{B}}(t_{\mathcal{S}}s_1(a - 1_{\mathcal{B}})) = k$ . So

$$\|r(a) - s_1(a)\|_{\mathcal{B},\infty} = |f_{\mathcal{B}}(r(a)) - f_{\mathcal{B}}(s_1(a))| = \left|k - \frac{p}{2}\right| = |k - k| = 0.$$

If  $p$  is odd, then  $p = 2k - 1$  for some  $k \in \mathbb{Z}$ , and  $f_{\mathcal{B}}(r(a)) = f_{\mathcal{B}}(t_{\mathcal{S}}s_1(a - 1_{\mathcal{B}})) = k - 1$ . Hence,  $\|r(a) - s_1(a)\|_{\mathcal{B},\infty} = |f_{\mathcal{B}}(r(a)) - f_{\mathcal{B}}(s_1(a))| = |k - 1 - \frac{p}{2}| = \frac{1}{2}$ .  $\square$

Thus, by replacing  $s_1(\cdot)$  by  $r(\cdot)$  in Table 2, we obtain the analogous lossy operators, denoted  $\tilde{L}$  and  $\tilde{L}^{-1}$ , outlined in Table 3.

$\tilde{L}$			$\tilde{L}^{-1}$		
$\mathbf{a}_1 \leftarrow \mathbf{a}_1 + \mathbf{a}_4$	$\mathbf{a}_1 \leftarrow r(\mathbf{a}_1)$	$\mathbf{a}_4 \leftarrow \mathbf{a}_4 - \mathbf{a}_1$	$\mathbf{a}_2 \leftarrow \mathbf{a}_2 + r(\mathbf{a}_4)$	$\mathbf{a}_4 \leftarrow \mathbf{a}_4 - r(\mathbf{a}_2)$	
$\mathbf{a}_3 \leftarrow \mathbf{a}_3 + \mathbf{a}_2$	$\mathbf{a}_3 \leftarrow r(\mathbf{a}_3)$	$\mathbf{a}_2 \leftarrow \mathbf{a}_2 - \mathbf{a}_3$	$\mathbf{a}_2 \leftarrow \mathbf{a}_2 + \mathbf{a}_4$	$\mathbf{a}_4 \leftarrow s_{-1}(\mathbf{a}_4)$	$\mathbf{a}_4 \leftarrow \mathbf{a}_4 - \mathbf{a}_2$
$\mathbf{a}_1 \leftarrow \mathbf{a}_1 + \mathbf{a}_3$	$\mathbf{a}_1 \leftarrow r(\mathbf{a}_1)$	$\mathbf{a}_3 \leftarrow \mathbf{a}_3 - \mathbf{a}_1$	$\mathbf{a}_3 \leftarrow \mathbf{a}_3 + \mathbf{a}_1$	$\mathbf{a}_1 \leftarrow s_{-1}(\mathbf{a}_1)$	$\mathbf{a}_1 \leftarrow \mathbf{a}_1 - \mathbf{a}_3$
$\mathbf{a}_4 \leftarrow \mathbf{a}_4 + \mathbf{a}_2$	$\mathbf{a}_4 \leftarrow r(\mathbf{a}_4)$	$\mathbf{a}_2 \leftarrow \mathbf{a}_2 - \mathbf{a}_4$	$\mathbf{a}_2 \leftarrow \mathbf{a}_2 + \mathbf{a}_3$	$\mathbf{a}_3 \leftarrow s_{-1}(\mathbf{a}_3)$	$\mathbf{a}_3 \leftarrow \mathbf{a}_3 - \mathbf{a}_2$
$\mathbf{a}_4 \leftarrow \mathbf{a}_4 + r(\mathbf{a}_2)$	$\mathbf{a}_2 \leftarrow \mathbf{a}_2 - r(\mathbf{a}_4)$		$\mathbf{a}_4 \leftarrow \mathbf{a}_4 + \mathbf{a}_1$	$\mathbf{a}_1 \leftarrow s_{-1}(\mathbf{a}_1)$	$\mathbf{a}_1 \leftarrow \mathbf{a}_1 - \mathbf{a}_4$

Table 3: Bit arithmetic steps for the lossy implementation of ZFP's forward (left) and backward (right) transform.

Now that all the required notation and tools have been discussed, the following lemma establishes a forward error bound for  $\tilde{L}$ .

LEMMA 4.3. *Suppose  $\mathbf{x} \in \mathbb{Z}^4$  such that  $e_{\max}(\mathbf{x}) \geq q - 1$  and  $\mathbf{x} \neq \mathbf{0}$ . Given the bit arithmetic implementation in Table 2 and Table 3 for ZFP's forward linear transforms, we have*

$$\|L\mathbf{x} - \tilde{L}\mathbf{x}\|_{\infty} \leq \frac{7}{4}\epsilon_q\|\mathbf{x}\|_{\infty}.$$

*Proof.* First the action of  $L$  and  $\tilde{L}$  will be formed as a composite operator of each step, as depicted in Table 2 and 3, respectively. Then a bound on the error between the action of  $L$  and  $\tilde{L}$  will be constructed using the Lemma 4.2 and the triangle inequality. Define  $\mathbf{a} = [\mathbf{a}_1, \mathbf{a}_2, \mathbf{a}_3, \mathbf{a}_4]^T = F_{\mathcal{B}}^{-1}(\mathbf{x}) \in \mathcal{B}^4$  to be the representation of  $\mathbf{x}$  in  $\mathcal{B}^4$ . From Table 2, the lossless operator for the first two steps can be written as

$$\mathbf{a}_1 \leftarrow \mathbf{a}_1 + \mathbf{a}_4 \quad \Rightarrow \quad L_{\mathcal{B},1}(\mathbf{a}) = [\mathbf{a}_1 + \mathbf{a}_4, \mathbf{a}_2, \mathbf{a}_3, \mathbf{a}_4]^T,$$

and

$$\mathbf{a}_1 \leftarrow s_1(\mathbf{a}_1), \quad \Rightarrow \quad L_{\mathcal{B},2}(\mathbf{a}) = [s_1(\mathbf{a}_1), \mathbf{a}_2, \mathbf{a}_3, \mathbf{a}_4]^T,$$

where we write  $L_{\mathcal{B},i}$  to represent the action at the  $i$ th step of the operator  $L$  on an element of  $\mathcal{B}^4$  from Table 2. The composite operator for the first two steps can now be expressed as

$$L_{\mathcal{B},2} \circ L_{\mathcal{B},1}(\mathbf{a}) = [s_1(\mathbf{a}_1 + \mathbf{a}_4), \mathbf{a}_2, \mathbf{a}_3, \mathbf{a}_4]^t.$$

Let  $L_{\mathcal{B}}$  denote the action of  $L$  in the vector space  $\mathcal{B}^4$ . Continuing in the same manner as above, we have

$$\begin{aligned} L_{\mathcal{B}}\mathbf{a} &= L_{\mathcal{B},14} \circ \dots \circ L_{\mathcal{B},1}(\mathbf{a}), \\ &= \begin{bmatrix} s_1(s_1(\mathbf{a}_4 + \mathbf{a}_1) + s_1(\mathbf{a}_2 + \mathbf{a}_3)) \\ \mathbf{z} - s_1(\mathbf{z} + \mathbf{w}) - s_1(s_1(\mathbf{z} + \mathbf{w}) + s_1(\mathbf{z} - s_1(\mathbf{z} + \mathbf{w}))) \\ s_1(\mathbf{a}_2 + \mathbf{a}_3) - s_1(s_1(\mathbf{a}_4 + \mathbf{a}_1) + s_1(\mathbf{a}_2 + \mathbf{a}_3)) \\ s_1(\mathbf{z} + \mathbf{w}) + s_1(\mathbf{w} - s_1(\mathbf{z} + \mathbf{w})) \end{bmatrix}, \end{aligned}$$

where  $\mathbf{z} = \mathbf{a}_4 - s_1(\mathbf{a}_4 + \mathbf{a}_1)$  and  $\mathbf{w} = \mathbf{a}_2 - s_1(\mathbf{a}_2 + \mathbf{a}_3)$ . Next, from Table 3, we obtain the analogous lossy operator, denoted  $\tilde{L}_{\mathcal{B}}$ . By replacing  $s_1(\cdot)$  by  $r(\cdot)$  we obtain  $\tilde{L}_{\mathcal{B}}\mathbf{a}$ . Now

$$(4.8) \quad \|L\mathbf{x} - \tilde{L}\mathbf{x}\|_{\infty} = \|L_{\mathcal{B}}\mathbf{a} - \tilde{L}_{\mathcal{B}}\mathbf{a}\|_{\mathcal{B},\infty} = \max_{1 \leq i \leq 4} |f_{\mathcal{B}}((L_{\mathcal{B}}\mathbf{a})_i) - f_{\mathcal{B}}((\tilde{L}_{\mathcal{B}}\mathbf{a})_i)|.$$

In particular, we found that the maximum in (4.8) is attained for  $i = 2$ . Using Lemma 4.2 and using  $s_1(c) = f_{\mathcal{B}}^{-1}(f_{\mathcal{B}}(c)/2) = \frac{1}{2}c$  for all  $c \in \mathcal{B}$ , we derive the following bound. Letting  $\mathbf{y} = L_{\mathcal{B}}\mathbf{a}$  and  $\tilde{\mathbf{y}} = \tilde{L}_{\mathcal{B}}\mathbf{a}$ , we find that

$$\begin{aligned} (4.9) \quad \|\mathbf{y}_2 - \tilde{\mathbf{y}}_2\|_{\mathcal{B},1} &= \left\| \frac{1}{4}(\mathbf{a}_2 + \mathbf{a}_3 - \mathbf{a}_1 - \mathbf{a}_4) - [\mathbf{z} - s_1(\mathbf{z} + \mathbf{w}) - s_1(s_1(\mathbf{z} + \mathbf{w}) + s_1(\mathbf{z} - s_1(\mathbf{z} + \mathbf{w}))) \right\|_{\mathcal{B},1}, \\ &\leq \frac{1}{2} + \left\| \frac{1}{4}(\mathbf{a}_2 + \mathbf{a}_3 - \mathbf{a}_1 - \mathbf{a}_4) - \left[ \mathbf{z} - \frac{3}{2}s_1(\mathbf{z} + \mathbf{w}) - \frac{1}{2}s_1(\mathbf{z} - s_1(\mathbf{z} + \mathbf{w})) \right] \right\|_{\mathcal{B},1}, \\ &\leq \frac{1}{2} + \frac{1}{4} + \left\| \frac{1}{4}(\mathbf{a}_2 + \mathbf{a}_3 - \mathbf{a}_1 - \mathbf{a}_4) - \left[ \frac{3}{4}\mathbf{z} - \frac{5}{4}s_1(\mathbf{z} + \mathbf{w}) \right] \right\|_{\mathcal{B},1}, \\ &\leq \frac{1}{2} + \frac{1}{4} + \frac{5}{8} + \left\| \frac{1}{4}(\mathbf{a}_2 + \mathbf{a}_3 - \mathbf{a}_1 - \mathbf{a}_4) - \left[ \frac{1}{8}\mathbf{z} - \frac{5}{8}\mathbf{w} \right] \right\|_{\mathcal{B},1}, \\ &\leq \frac{1}{2} + \frac{1}{4} + \frac{5}{8} + \frac{1}{16} + \frac{5}{16} = \frac{28}{16} \end{aligned}$$

where (4.9) follows from the triangle inequality and Lemma 4.2. Similarly,  $\|\mathbf{y}_i - \tilde{\mathbf{y}}_i\|_{\mathcal{B},1} \leq \frac{28}{16}$ , for all  $1 \leq i \leq 4$ . Since  $\|\mathbf{x}\|_{\infty} \geq 2^{q-1}$ , it now follows that

$$\|L\mathbf{x} - \tilde{L}\mathbf{x}\|_{\infty} \leq \frac{28}{16} 2^{-q+1} \|\mathbf{x}\|_{\infty} = \frac{7}{4} \epsilon_q \|\mathbf{x}\|_{\infty}.$$

□

The following result extends the 1- $d$  error caused by the lossy forward transform operator established in Lemma 4.3 to  $d$  dimensions.

LEMMA 4.4. *Suppose  $\mathbf{x} \in \mathbb{Z}^{4^d}$  such that  $e_{\max, \mathcal{B}}(\mathbf{x}) = q$ . Then*

$$\|L_d\mathbf{x} - \tilde{L}_d\mathbf{x}\|_{\infty} \leq k_L \epsilon_q \|\mathbf{x}\|_{\infty},$$

where  $k_L = \frac{7}{4}(2^d - 1)$ .

*Proof.* Let  $\Delta L$  represent a perturbation of the action of  $L$  such that  $\tilde{L} = L + \Delta L$ . From Lemma 4.3, we have  $\|\Delta L \mathbf{y}\|_\infty \leq \frac{7}{4} \epsilon_q \|\mathbf{y}\|_\infty$ , for all  $\mathbf{y} \in \{\mathbf{z} \in \mathbb{Z}^4 : e_{max}(\mathbf{z}) \geq q - 1\}$ . Hence,

$$\|(I_{4^d} \otimes \Delta L) \mathbf{x}\|_\infty = \|(\Delta L \otimes I_{4^d}) \mathbf{x}\|_\infty \leq \frac{7}{4} \epsilon_q \|\mathbf{x}\|_\infty.$$

Using the inequalities  $\|\Delta L\|_\infty \leq 1$  and  $\|L\|_\infty = 1$ , we have

$$\begin{aligned} \|L_d \mathbf{x} - \tilde{L}_d \mathbf{x}\|_\infty &= \|(L \otimes \dots \otimes L) \mathbf{x} - ((L + \Delta L) \otimes \dots \otimes (L + \Delta L)) \mathbf{x}\|_\infty, \\ &\leq \left( \sum_{i=1}^d \binom{d}{i} \|L\|_\infty^{d-i} \|\Delta L\|_\infty^{i-1} \right) \frac{7}{4} \epsilon_q \|\mathbf{x}\|_\infty, \\ &= \frac{7}{4} \left( \sum_{i=1}^d \binom{d}{i} \right) \epsilon_q \|\mathbf{x}\|_\infty, \\ &= \frac{7}{4} (2^d - 1) \epsilon_q \|\mathbf{x}\|_\infty. \end{aligned}$$

□

At this point, it remains to consider ZFP's backward linear transform with respect to Table 2 and Table 3. For this particular implementation of ZFP, if Steps 3 through 8 of the compression algorithm are applied before the backwards transform, no additional error occurs<sup>1</sup>. The decompression operator for the particular implementation of ZFP is defined as the corresponding lossless operator

$$\tilde{D}_3(\mathbf{a}) = D_3(\mathbf{a}) = F_B^{-1} L_d^{-1} F_B(\mathbf{a}), \text{ for all } \mathbf{a} \in \mathcal{B}^{4^d}.$$

**4.4. Reorder coefficients by total sequency.** The fourth step performs a deterministic permutation on the components of the input. As such, it is an invertible operation. We define  $C_4 : \mathcal{B}^{4^d} \rightarrow \mathcal{B}^{4^d}$  to be the map that takes the components of a block in row-major order and permutes them so that the resulting block is in total sequency order [16]. The decompression operator performs the inverse permutation such that  $D_4 C_4(\mathbf{a}) = \mathbf{a}$ , for all  $\mathbf{a} \in \mathcal{B}^{4^d}$ . We summarize the key details for these operators below.

PROPOSITION 4.5. *Suppose  $\mathbf{a} \in \mathcal{B}^{4^d}$ . Then  $\|C_4(\mathbf{a})\|_{\mathcal{B},p} = \|\mathbf{a}\|_{\mathcal{B},p} = \|D_4(\mathbf{a})\|_{\mathcal{B},p}$ , for all  $1 \leq p \leq \infty$ .*

**4.5. Convert signed two's complement to negabinary.** At Step 5 of the algorithm, each component is converted from its two's complement representation to a negabinary representation. As we are representing values using a signed binary representation instead of a two's complement representation for our analysis, we will need to convert each signed binary representation to a negabinary representation. Using the operators defined in Section 3, we define the operator  $C_5 : \mathcal{B}^{4^d} \rightarrow \mathcal{N}^{4^d}$  by

$$C_5(\mathbf{a}) := F_{\mathcal{N}}^{-1} F_B(\mathbf{a}), \text{ for all } \mathbf{a} \in \mathcal{B}^{4^d}.$$

A valid concern for this step is that the range of representable integers for an  $N$ -bit two's complement representation is not the same as the range of representable integers for an  $N$ -bit negabinary

<sup>1</sup>The first two steps of the backwards transform operator, depicted in Table 3, may result in round-off. However, the additional error that may occur depends on the user-defined parameters that define the action of Step 8. If Step 8 is performed losslessly, i.e., no bit planes are discarded, then each step of the backward transform, in bit arithmetic, undoes the associated step of the forward transform. If at least  $2d$  bit planes are discarded at Step 8 (see Section 4.8 for details), then the first two steps of the backwards transform will not introduce additional error. If between 1 and  $2d - 1$  bit planes are discarded, additional error may occur in the decompression step. However, since ZFP will result in a low compression ratio if only between 1 and  $2d - 1$  bit planes are discarded, the remainder of the paper will assume at least  $2d$  bit planes are discarded. See Appendix B for details.

representation, for any integer  $N \geq 2$ . To account for this difference, ZFP uses an  $(N - 1)$ -bit two's complement representation with one bit left unused, called a guard bit. In Step 3, the guard bit was required for the decorrelating transform but is unnecessary for the remaining steps. Thus, when the two's complement representation is converted to a negabinary representation in ZFP the guard bit is freed and used instead for an  $N$ -bit negabinary representation to ensure that the integer can be represented. Additionally, since the magnitude of each component is not increased in the following steps, the components can be converted back to two's complement without introducing any error due to round off. Hence, Step 5 is lossless. Lastly, it follows that the decompression operator is defined as  $D_5 := F_B^{-1}F_N$ . The following result summarizes the key result from this step used in the analysis in Section 5.

**PROPOSITION 4.6.** *Suppose  $\mathbf{a} \in \mathcal{B}_k^n$ . Then  $\|C_5(\mathbf{a})\|_{\mathcal{N},p} = \|\mathbf{a}\|_{\mathcal{B},p}$  for all  $1 \leq p \leq \infty$ .*

**4.6. Boolean matrix transposition.** Next, the bit vectors are reordered by their bit index instead of their associated binary representation. Under the bit vector representation, this corresponds to transposing the entire block. Since this operation is lossless and does not result in altering the representation of any element in the block, we do not define an operator here. For simplicity, we will work under the assumption that the transposition did not take place.

**4.7. Embedded block coding.** In Step 7, each bit plane of  $4^d$  bits is individually coded with a variable-length code that is one to one and reversible (see [16] for details). For purposes of the analysis, since Step 7 is lossless, we chose not to consider the encoding in Step 7 since the error analysis can be considered in any format. Hence, for the purposes of simplifying the analysis, we take  $C_7 = D_7 = I_N$ .

**4.8. Finite-precision: Bit stream truncation.** Step 8 is dependent on one parameter, denoted  $\beta \geq 0$ , and an index set dependent on  $\beta$  and the input, denoted as  $\mathcal{P}$ . Here,  $\beta$  represents the number of most significant bit planes to keep during Step 8 and any discarded bit plane is replaced with all-zero bits. Note that the value of  $\beta$  corresponds to the parameter `zfp_stream.maxprec` in ZFP and can be set to any positive integer by the user in the fixed precision mode of ZFP. The operator for Step 8 is given by  $\tilde{C}_8 : \mathcal{N}^{4^d} \rightarrow \mathcal{N}^{4^d}$  and defined as

$$\tilde{C}_8(\mathbf{d}) := T_{\mathcal{P}}(\mathbf{d}), \text{ for all } \mathbf{d} \in \mathcal{N}^{4^d},$$

where  $\mathcal{P} = \{i \in \mathbb{Z} : i > q + 1 - \beta\}$ ,  $q \in \mathbb{N}$  is the value from Step 2, and  $T_{\mathcal{P}}$  is the truncation operator with respect to set  $\mathcal{P}$ . The lossless compression and decompression operators are then defined by  $C_8 := I_N$  and  $D_8 := I_N$ , respectively. We conclude this step with a proposition that immediately follows from Lemma 3.7.

**PROPOSITION 4.7.** *Suppose  $\mathbf{a} \in \mathcal{B}^{4^d}$  such that  $F_B(\mathbf{a}) \in \mathbb{Z}^{4^d}$  and  $e_{max,\mathcal{B}}(F_B(\mathbf{a})) \geq q - 1$ . Then  $\|\tilde{C}_8 C_5 \mathbf{a} - C_8 C_5 \mathbf{a}\|_{\mathcal{N},\infty} \leq \frac{8}{3} \epsilon_{\beta} \|\mathbf{a}\|_{\mathcal{B},\infty}$ .*

*Proof.* Let  $\mathbf{d} = C_5 \mathbf{a}$ . From Lemma 3.7 (ii) we have that

$$(4.10) \quad \|\tilde{C}_8 \mathbf{d} - C_8 \mathbf{d}\|_{\mathcal{N},\infty} = \|T_{\mathcal{P}} \mathbf{d} - \mathbf{d}\|_{\mathcal{N},\infty} \leq \frac{2}{3} \epsilon_{\beta} 2^{q+1}.$$

From the assumption  $e_{max,\mathcal{B}}(F_B(\mathbf{a})) \geq q - 1$  it now follows that  $\|\mathbf{a}\|_{\infty} \geq 2^{q-1}$  and

$$\|\tilde{C}_8 C_5 \mathbf{a} - C_8 C_5 \mathbf{a}\|_{\mathcal{N},\infty} \leq \frac{8}{3} \epsilon_{\beta} \|\mathbf{a}\|_{\infty}. \quad \square$$

To conclude this section, it should be noted that the inputs at Step 5 of ZFP satisfy the hypotheses of Proposition 4.7 as each component is encoded as an integer up to precision  $q$ .

**4.9. Defining the ZFP Compression Operator.** To conclude this section, we define the ZFP fixed precision compression and decompression operators by composing the operators defined for each step of the algorithm. In order to simplify the definition of each operator, we omit  $C_7$ ,  $D_7$ ,  $C_8$ , and  $D_8$  from the composition, as they were defined to be the identity operator  $I_N$ .

DEFINITION 4.8. *The lossy fixed precision compression operator,  $\tilde{C} : \mathbb{R}^{4^d} \rightarrow \mathcal{N}^{4^d}$ , is defined by*

$$\tilde{C}(\mathbf{x}) = \left( \tilde{C}_8 \circ C_5 \circ C_4 \circ \tilde{C}_3 \circ \tilde{C}_2 \right) (\mathbf{x}), \quad \text{for all } \mathbf{x} \in \mathbb{R}^{4^d},$$

where  $\circ$  denotes the usual composition of operators. The lossless fixed precision compression operator,  $C : \mathbb{R}^{4^d} \rightarrow \mathcal{N}^{4^d}$ , is defined by

$$C(\mathbf{x}) = (C_5 \circ C_4 \circ C_3 \circ C_2) (\mathbf{x}), \quad \text{for all } \mathbf{x} \in \mathbb{R}^{4^d}.$$

Lastly, the lossy fixed precision decompression operator,  $\tilde{D} : \mathcal{N}^{4^d} \rightarrow \mathbb{R}^{4^d}$ , is defined by

$$\tilde{D}(\mathbf{d}) = \left( \tilde{D}_2 \circ D_3 \circ D_4 \circ D_5 \right) (\mathbf{d}), \quad \text{for all } \mathbf{d} \in \mathcal{N}^{4^d},$$

and the the lossless fixed precision decompression operator  $D : \mathcal{N}^{4^d} \rightarrow \mathbb{R}^{4^d}$  is defined by

$$D(\mathbf{d}) = (D_2 \circ D_3 \circ D_4 \circ D_5) (\mathbf{d}), \quad \text{for all } \mathbf{d} \in \mathcal{N}^{4^d}.$$

**5. Error Bounds for ZFP Compression and Decompression.** Now that the ZFP fixed precision compression and decompression operators have been defined, we can establish a bound on the forward error for an arbitrary input that is compressed and decompressed. We begin by analyzing the error introduced during compression. Recall that  $\beta$  is the fixed precision parameter, i.e.,  $\beta$  bits for each of the ZFP transform coefficients will be kept during compression.

LEMMA 5.1. *Assume  $\mathbf{x} \in \mathbb{R}^{4^d}$  with  $\mathbf{x} \neq \mathbf{0}$  such that  $F_{\mathcal{B}}^{-1}(\mathbf{x}) \in \mathcal{B}_k^{4^d}$ , for some precision  $k$ . Let  $\beta \geq 0$  be the fixed precision parameter. Then*

$$\|\tilde{C}\mathbf{x} - C\mathbf{x}\|_{\mathcal{N},\infty} \leq 2^{-\ell} \left( \frac{8}{3}\epsilon_{\beta} + \epsilon_q \left( 1 + \frac{8}{3}\epsilon_{\beta} \right) (k_L(1 + \epsilon_q) + 1) \right) \|\mathbf{x}\|_{\infty},$$

where  $q \in \mathbb{N}$  is the precision for the block-floating point representation in Step 2,  $\ell = e_{\max, \mathcal{B}}(\mathbf{x}) - q + 1$ , and  $k_L = \frac{7}{4}(2^d - 1)$ .

*Proof.* Define  $c(\mathbf{x}) := \|\tilde{C}\mathbf{x} - C\mathbf{x}\|_{\mathcal{N},\infty}$ . First, we find that

$$\begin{aligned} c(\mathbf{x}) &= \|\tilde{C}_8 C_5 C_4 \tilde{C}_3 \tilde{C}_2 \mathbf{x} - C\mathbf{x}\|_{\mathcal{N},\infty}, \\ &= \|\tilde{C}_8 C_5 C_4 \tilde{C}_3 \tilde{C}_2 \mathbf{x} - C_5 C_4 \tilde{C}_3 \tilde{C}_2 \mathbf{x} + C_5 C_4 \tilde{C}_3 \tilde{C}_2 \mathbf{x} - C\mathbf{x}\|_{\mathcal{N},\infty}, \\ &\leq \|\tilde{C}_8 C_5 C_4 \tilde{C}_3 \tilde{C}_2 \mathbf{x} - C_5 C_4 \tilde{C}_3 \tilde{C}_2 \mathbf{x}\|_{\mathcal{N},\infty} + \|C_5 C_4 \tilde{C}_3 \tilde{C}_2 \mathbf{x} - C\mathbf{x}\|_{\mathcal{N},\infty}. \end{aligned}$$

By the definition of  $C_4$  and  $C_5$ , we have  $\|C_5 C_4 \tilde{C}_3 \tilde{C}_2 \mathbf{x} - C\mathbf{x}\|_{\mathcal{N},\infty} = \|\tilde{C}_3 \tilde{C}_2 \mathbf{x} - C_3 C_2 \mathbf{x}\|_{\mathcal{B},\infty}$ . Additionally,  $\|\tilde{C}_8 C_5 C_4 \tilde{C}_3 \tilde{C}_2 \mathbf{x} - C_5 C_4 \tilde{C}_3 \tilde{C}_2 \mathbf{x}\|_{\mathcal{N},\infty} \leq 8\epsilon_{\beta} \|\tilde{C}_3 \tilde{C}_2 \mathbf{x}\|_{\mathcal{B},\infty}$  follows by applying Proposition 4.7 and the definition of  $C_4$ . Hence,

$$\begin{aligned} c(\mathbf{x}) &\leq 8\epsilon_{\beta} \|\tilde{C}_3 \tilde{C}_2 \mathbf{x}\|_{\mathcal{B},\infty} + \|\tilde{C}_3 \tilde{C}_2 \mathbf{x} - C_3 C_2 \mathbf{x}\|_{\mathcal{B},\infty}, \\ &\leq \left( 1 + \frac{8}{3}\epsilon_{\beta} \right) \|\tilde{C}_3 \tilde{C}_2 \mathbf{x} - C_3 \tilde{C}_2 \mathbf{x}\|_{\mathcal{B},\infty} + \frac{8}{3}\epsilon_{\beta} \|C_3 \tilde{C}_2 \mathbf{x}\|_{\mathcal{B},\infty} + \|C_3 \tilde{C}_2 \mathbf{x} - C_3 C_2 \mathbf{x}\|_{\mathcal{B},\infty}, \\ &\leq \left( 1 + \frac{8}{3}\epsilon_{\beta} \right) \|\tilde{C}_3 \tilde{C}_2 \mathbf{x} - C_3 \tilde{C}_2 \mathbf{x}\|_{\mathcal{B},\infty} + \frac{8}{3}\epsilon_{\beta} \|\tilde{C}_2 \mathbf{x}\|_{\mathcal{B},\infty} + \|\tilde{C}_2 \mathbf{x} - C_2 \mathbf{x}\|_{\mathcal{B},\infty}, \end{aligned}$$

where the final inequality follows from the linearity of  $C_3$  and  $\|C_3\|_{\mathcal{B},\infty} \leq 1$ . By the definition of  $\tilde{C}_2$ , we have that  $e_{\max, \mathcal{B}}(\tilde{C}_2 \mathbf{x}) \geq q - 1$ . Hence, Lemma 4.4 yields that  $\|\tilde{C}_3 \tilde{C}_2 \mathbf{x} - C_3 \tilde{C}_2 \mathbf{x}\|_{\mathcal{B},\infty} \leq k_L \epsilon_q \|\tilde{C}_2 \mathbf{x}\|_{\mathcal{B},\infty}$ . Lastly, using Proposition 4.1, we have that  $\|\tilde{C}_2 \mathbf{x} - C_2 \mathbf{x}\|_{\mathcal{B},\infty} \leq 2^{-\ell} \epsilon_q \|\mathbf{x}\|_{\infty}$ , which yields the inequality  $\|\tilde{C}_2 \mathbf{x}\|_{\mathcal{B},\infty} \leq 2^{-\ell} (1 + \epsilon_q) \|\mathbf{x}\|_{\infty}$ . Combining these observations provides the desired result.  $\square$



The following result provides bound on the error resulting from compressing then decompressing a  $4^d$  block using ZFP.

**THEOREM 5.2.** *Assume  $\mathbf{x} \in \mathbb{R}^{4^d}$  with  $\mathbf{x} \neq \mathbf{0}$  such that  $F_{\mathcal{B}}(\mathbf{x}) \in \mathcal{B}_k^{4^d}$ , for some precision  $k$ . Let  $0 \leq \beta \leq q - 2d + 2$  be the fixed precision parameter.<sup>2</sup> Then*

$$(5.1) \quad \|\tilde{D}\tilde{C}\mathbf{x} - \mathbf{x}\|_{\infty} \leq K_{\beta}\|\mathbf{x}\|_{\infty}$$

where  $q \in \mathbb{N}$  is the precision for the block-floating point representation in Step 2,

$$(5.2) \quad K_{\beta} := \left(\frac{15}{4}\right)^d \left( (1 + \epsilon_k) \left( \frac{8}{3}\epsilon_{\beta} + \epsilon_q \left( 1 + \frac{8}{3}\epsilon_{\beta} \right) (k_L(1 + \epsilon_q) + 1) \right) + \epsilon_k \right),$$

and  $k_L = \frac{7}{4}(2^d - 1)$ .

*Proof.* Observe that

$$(5.3) \quad \begin{aligned} \|\tilde{D}\tilde{C}\mathbf{x} - D\mathbf{C}\mathbf{x}\|_{\infty} &= \|\tilde{D}_2 D_3 D_4 D_5 \tilde{C}\mathbf{x} - D_2 D_3 D_4 D_5 C\mathbf{x}\|_{\infty}, \\ &\leq \|\tilde{D}_2 D_3 D_4 D_5 \tilde{C}\mathbf{x} - D_2 D_3 D_4 D_5 \tilde{C}\mathbf{x}\|_{\infty} + \|D_2 D_3 D_4 D_5 \tilde{C}\mathbf{x} - D_2 D_3 D_4 D_5 C\mathbf{x}\|_{\infty}, \\ &\leq 2^{\ell} \epsilon_k \|D_3 D_4 D_5 \tilde{C}\mathbf{x}\|_{\mathcal{B}, \infty} + \|D_2 D_3 D_4 D_5\| \|\tilde{C}\mathbf{x} - C\mathbf{x}\|_{\mathcal{N}, \infty}, \end{aligned}$$

$$(5.4) \quad \leq 2^{\ell} \left(\frac{15}{4}\right)^d \left( \epsilon_k \|\tilde{C}\mathbf{x}\|_{\mathcal{N}, \infty} + \|\tilde{C}\mathbf{x} - C\mathbf{x}\|_{\mathcal{N}, \infty} \right),$$

$$(5.5) \quad \leq 2^{\ell} \left(\frac{15}{4}\right)^d \left( (1 + \epsilon_k) \|\tilde{C}\mathbf{x} - C\mathbf{x}\|_{\mathcal{N}, \infty} + \epsilon_k \|C\mathbf{x}\|_{\mathcal{N}, \infty} \right),$$

$$(5.5) \quad \leq 2^{\ell} \left(\frac{15}{4}\right)^d \left( (1 + \epsilon_k) \|\tilde{C}\mathbf{x} - C\mathbf{x}\|_{\mathcal{N}, \infty} + 2^{-\ell} \epsilon_k \|\mathbf{x}\|_{\infty} \right),$$

where (5.3) follows from Proposition 4.1(ii) and (5.4) follows from the linearity of  $D_2$ ,  $D_3$ ,  $D_4$ , and  $D_5$  and  $\ell = e_{\max, \mathcal{B}}(\mathbf{x}) - q + 1$ . Applying Lemma 5.1 in (5.5) yields the desired result.  $\square$

Since the constant  $K_{\beta}$  appears in the bound, which is dependent on  $k$ ,  $q$ ,  $d$ , and  $\beta$ , we provide a brief discussion on  $K_{\beta}$  in Appendix C. Note that Theorem 5.2 yields the following bound on the maximum of the component-wise relative error:

$$(5.6) \quad \max_{i, \mathbf{x}_i \neq 0} \left| \frac{(\tilde{D}\tilde{C}\mathbf{x})_i - \mathbf{x}_i}{\mathbf{x}_i} \right| \leq \frac{1}{\min_{i, \mathbf{x}_i \neq 0} |\mathbf{x}_i|} \|\tilde{D}\tilde{C}\mathbf{x} - \mathbf{x}\|_{\infty} \leq K_{\beta} 2^{e_{\max, \mathcal{B}}(\mathbf{x}) - e_{\min, \mathcal{B}}(\mathbf{x})}.$$

So far, the discussion and error analysis has focused on the fixed precision mode. However, as mentioned during the introduction, ZFP also has a fixed accuracy and fixed rate mode. While we will not spend much time providing details for the fixed accuracy and fixed rate modes, it should be noted that the error bound in Theorem 5.2 allows us to develop error bounds for the fixed accuracy and fixed rate modes.

In the fixed accuracy mode, the transform coefficients in each  $4^d$  block are encoded up to a minimum bit plane number. The index of the minimum bit plane will be dependent on the largest absolute magnitude and the constant  $K_{\beta}$  found in Theorem 5.2. The following theorem is an extension of Theorem 5.2 for fixed accuracy mode of ZFP.

<sup>2</sup>In other words, it is assumed that at least  $2d$  least significant bit planes are discarded in Step 8. If less than  $2d$  bit planes are discarded, i.e.,  $q - 2d + 2 < \beta < q + 2$ , error will occur in Step 3 from round-off that may occur by the decompression operator, which is not taken into account in Theorem 5.2. Theorem B.2 is the generalization of Theorem 5.2 for the assumption  $q - 2d + 2 < \beta < q + 2$ . See Appendix B for details.

**THEOREM 5.3.** *Assume  $\mathbf{x} \in \mathbb{R}^n$  with  $\mathbf{x} \neq \mathbf{0}$  such that  $F_{\mathcal{B}}(\mathbf{x}) \in \mathcal{B}_k^n$ , for some precision  $k$  and let  $\hat{\mathbf{x}}$  represent the compressed and decompressed values from using the fixed accuracy mode of ZFP. To guarantee  $b \in \mathbb{N}$  bits of accuracy, i.e.,  $\|\hat{\mathbf{x}} - \mathbf{x}\|_{\infty} \leq 2^{-b}$ ,  $\beta$  must satisfy:*

$$(5.7) \quad \beta \geq \log_2 \left( \frac{\frac{16}{3}(1+c)}{\left(\frac{4}{15}\right)^d 2^{-b-e_{max}} - \epsilon_k} - c}{(1+\epsilon_k)} \right),$$

where  $c = \epsilon_q(k_L(1+\epsilon_q)+1)$  and  $e_{max} := e_{max}(\mathbf{x})$ .

*Proof.* Let  $\mathbf{x}^i$  denote the  $i$ -th  $4^d$  block of the  $d$ -dimensional data  $\mathbf{x} \in \mathbb{R}^n$ . Then we have that  $e_{max} := e_{max}(\mathbf{x}) = \max_i e_{max}(\mathbf{x}^i)$ . From the hypothesis it follows that  $K_{\beta} \leq 2^{-b-e_{max}}$ . From Theorem 5.2 and the fact that  $\|\mathbf{x}^i\|_{\infty} \geq 2^{e_{max}}$  for all  $i$ , we conclude that

$$\|\hat{\mathbf{x}} - \mathbf{x}\|_{\infty} = \max_i \|\tilde{D}\tilde{C}\mathbf{x}^i - \mathbf{x}^i\|_{\infty} \leq \max_i K_{\beta} \|\mathbf{x}^i\|_{\infty} \leq 2^{-b}. \quad \square$$

If we assume  $k = q = \infty$ , i.e., infinite precision, then Equation (5.7) simplifies to

$$(5.8) \quad \beta \geq \log_2 \left( \left( \frac{15}{4} \right)^d \frac{16}{3} 2^{b+e_{max}} \right).$$

Similarly, an upper bound for the fixed rate mode of ZFP can be obtained using Theorem 5.2. For the purposes of understanding the following result, it suffices to know that for the fixed rate mode of ZFP the user provides a maximum rate, denoted  $r$ , or number of bits per value to be stored.

**THEOREM 5.4.** *Assume  $\mathbf{x} \in \mathbb{R}^{4^d}$  with  $\mathbf{x} \neq \mathbf{0}$  such that  $F_{\mathcal{B}}(\mathbf{x}) \in \mathcal{B}_k^{4^d}$ , for some precision  $k$ . Let  $b_e$  be the number of bits to encode the exponent and let  $\hat{\mathbf{x}}$  represent the compressed and decompressed values in the fixed rate mode with rate,  $r \in \mathbb{N}$ . For some  $\beta \in \mathbb{N}$ , if*

$$\|\hat{\mathbf{x}} - \mathbf{x}\|_{\infty} \leq K_{\beta} \|\mathbf{x}\|,$$

then  $r \geq \frac{4^d \beta + b_e}{4^d} + 1$ .

*Proof.* In the worst case scenario, the first bit plane is all-ones, which would imply  $4^d - 1$  positive group tests (see [16] for details) and thus,  $4^d - 1$  bits to encode the the group tests. Each bit plane would then take  $4^d$  bits to encode. Note that, ZFP uses one bit to indicate if the block is all zeros. Thus, if given rate  $r$ , there is a total of  $4^d r$  bits that can be used to encode the block,  $b_e$  of those bits must be used to encode the block floating-point exponent in Step 2, one bit is used for the leading all-zeros bit and  $4^d - 1$  bits for the group testing, leaving  $(4^d r - b_e - 1 - (4^d - 1))$  bits to encode the bit planes. Implying

$$(5.9) \quad \beta \leq \frac{(4^d(r-1) - b_e)}{4^d} \Rightarrow r \geq \frac{4^d \beta + b_e}{4^d} + 1. \quad \square$$

Now that we have established bounds on the error introduced by ZFP compression and decompression, we consider several numerical experiments in order to observe the tightness of these bounds.

**6. Numerical Experiments.** In the following numerical tests, we consider two types of error, which we will refer to as *block relative error* and *componentwise relative error*, and their respective bounds:

$$\begin{aligned} \text{Block Relative Error: } & \frac{\|\tilde{D}\tilde{C}\mathbf{x} - \mathbf{x}\|_{\infty}}{\|\mathbf{x}\|_{\infty}} \leq K_{\beta}, \\ \text{Componentwise Relative Error: } & \max_{i, \mathbf{x}_i \neq 0} \frac{|\tilde{D}\tilde{C}\mathbf{x}_i - \mathbf{x}_i|}{|\mathbf{x}_i|} \leq K_{\beta} 2^{e_{max} - e_{min}}. \end{aligned}$$

As observed in Section 4, Steps 2, 3, and 8 of ZFP are the sources of round-off error. So, in constructing our numerical tests, we considered what conditions will vary the round-off error at these steps. Information is only lost in Step 2, if, when the block is converted from floating-point to block-floating-point, the exponent range of components in the block is above some threshold, as can be seen in equation (3.9). At Step 3, a linear transform is applied to the block, and information is lost whenever round-off occurs. At Step 8, if the number of compressed bit-planes does not coincide with the negabinary precision, we will again lose information. Since varying the exponent range of the input is an easy parameter to control, the value  $e_{\max} - e_{\min}$  is used as a parameter in many of the numerical tests. Additionally, we chose to vary the number of bit planes kept in Step 8, denoted  $\beta$ , in the following numerical experiments.

The first numerical experiment is designed to test how well the bound established in Section 5 captures the round-off error introduced by ZFP as the range of exponents and the number of bit-planes varies within a single block with dimension  $d$ . While the first test works on data generated to demonstrate the worst-case behavior, the second experiment shows the behavior for a data set taken from an actual physical simulation.

**6.1. Generated  $4^d$  Block.** In the first numerical test, a 4 by 4 block was formed with absolute values ranging from  $2^{e_{\min}}$  to  $2^{e_{\max}}$ . The exponent  $e_{\min}$  remains stationary while  $e_{\max}$  varies, depending on the chosen exponent range. The interval  $[e_{\min}, e_{\max}]$  was divided into 16 evenly spaced subintervals. Each value of the block was randomly selected from a uniform distribution in the range  $[2^{e_{\min}+(h-1)\frac{e_{\max}-e_{\min}}{16}}, 2^{e_{\min}+h\frac{e_{\max}-e_{\min}}{16}}]$  with subinterval  $h \in \{1, \dots, 16\}$  and uniform randomly assigned sign. The block was then randomly permuted, using the C++ standard library function *random\_shuffle*, to remove any bias in the total sequency order and then compressed and decompressed with precision,  $\beta$ . This specific construction of data is designed to mimic the worst possible input for ZFP for a chosen exponent range. For a given exponent range,  $\rho = e_{\max} - e_{\min}$ , we expect the componentwise relative error and block relative error to increase as the precision decreases. However, as the bound is only dependent on  $\beta$ , the block relative error bound will remain constant as the exponent range varies. The componentwise relative error should increase as the exponent range increases as the representable numbers in a block-floating-point representation are dependent on the largest exponent of the block and the value of  $q$ .

For Figures 4-5, the data is represented and compressed in single-precision (32-bit IEEE standard) with  $e_{\min} = 0$ , while  $e_{\max}$  varies with respect to the required exponent range. Similar results can be produced for any value of  $e_{\min}$ . Figure 4 shows how the componentwise relative error (top) and block relative error (bottom) vary with respect to the fixed precision parameter,  $\beta$ , for a fixed exponent range. For a single  $\beta$ , one decompressed. The blue band represents the sampled maximum and minimum of the true componentwise relative error or block relative error, i.e.,

$$\max_{i, \mathbf{x}_i \neq 0} \frac{|\tilde{D}\tilde{C}\mathbf{x}_i - \mathbf{x}_i|}{|\mathbf{x}_i|} \quad \text{and} \quad \frac{\|\tilde{D}\tilde{C}\mathbf{x} - \mathbf{x}\|_{\infty}}{\|\mathbf{x}\|_{\infty}},$$

respectively, of all 1 million runs. The red line depicts the theoretical bound and the dashed green line represents the asymptotic behavior of the bound, i.e., the smallest predictive value of the theoretical bound. For  $e_{\max} - e_{\min} = 0$ , meaning that the magnitude of the absolute values of the 4 by 4 block are similar, the componentwise relative error increases as  $\beta$  decreases. As the exponent range increases, fewer bits will be used to represent the smaller values in each block during Step 2 of ZFP, which will result in a larger relative error. As anticipated, in Figure 4 the entire plot shifts toward the upper right corner as the exponent range increases, indicating that the componentwise relative error increases with respect to the range of compressed values. With respect to the block relative error, the block relative error remains the same for all  $\beta$  as the exponent range varies.

Similar trends can also be seen in Figure 5, where the exponent range varies for a single  $\beta$ . In Figure 5, for each  $\beta$ , the componentwise relative error (top) increases as the exponent range increases while the block relative error remains constant, as expected. As  $\beta$  increases, both the componentwise

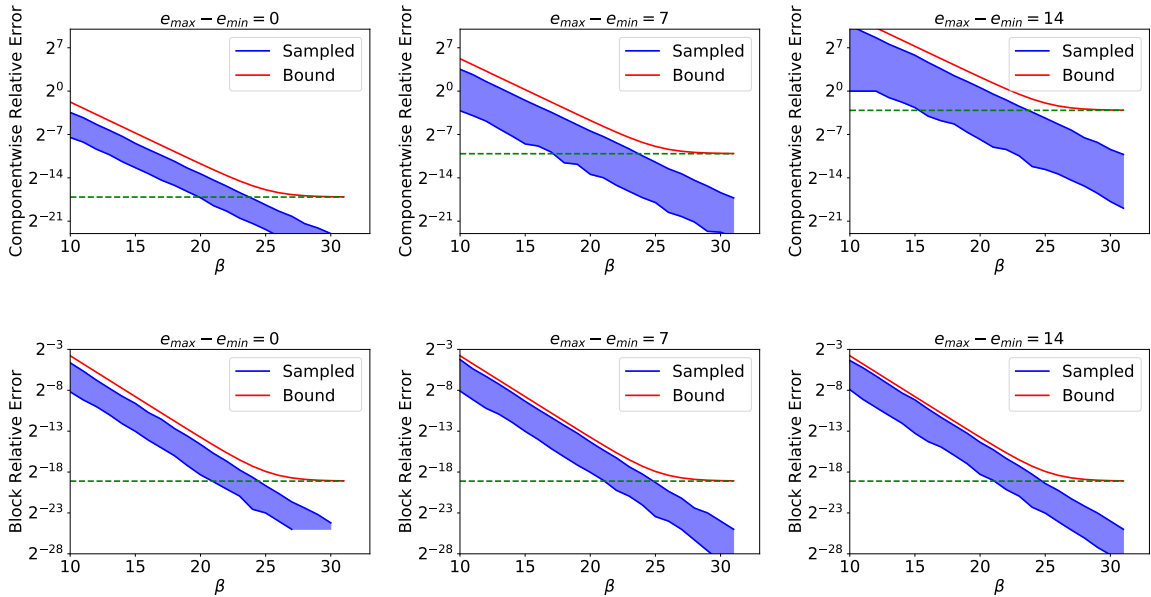


Fig. 4: 2-d Example with single precision: componentwise relative error (top) and block relative error (bottom) with respect to the precision parameter ( $\beta$ ) for  $e_{max} - e_{min} \in \{0, 7, 14\}$ . The blue band represents the sampled maximum and minimum error, the red line depicts the theoretical bound, and the dashed green line represents the asymptotic behavior of the theoretical bound.

relative error and the block relative error plots are shifted upwards, indicating an increase in error. For  $\beta = 32$ , there is a gap between the bound and the observed error, which corresponds to the gap in the far right of the plots in Figure 4, i.e., the theoretical error bound is limited to precision of the IEEE representation. It can be concluded, in Figures 4 and 5, that the theoretical bound (red) completely bounds the maximum sampled error (blue).

Next, we repeated this same experiment using a different machine precision. Note that Figures 6 and 7 represent the same two-dimensional test outlined above, but the values in the block are represented using double-precision (64-bit IEEE standard). The same relationships can be concluded for the double precision case.

Finally, since the dimensionality of the block plays an important part in ZFP, Figures 8 and 9 and Figures 10 and 11 represent results in double precision for one-dimensional and three-dimensional blocks, respectively. Again, similar relationships can be seen as those outlined in the two-dimensional, single-precision experiment.

**6.2. Real-World Example.** For this example, we compress data from a real-world three dimensional viscosity and density field from a Rayleigh-Taylor instability simulation produced by Miranda [5]. For the viscosity field, the average exponent range over all blocks is approximately 7.32. This data set is a highly variable example, as the viscosity values are signed and have a high dynamic range. The density field has a much smaller dynamic range than the viscosity field. That means the density field is a more compressible data set for ZFP. For both fields, the same value of  $\beta$  was used across all blocks during compression to simplify the visualization of the results. In Figure 12 and 13, the block relative error is plotted after the data has been compressed and decompressed (blue) as a function of  $\beta$ . The theoretical bound is plotted in red. Again, we conclude that the theoretical bound completely bounds

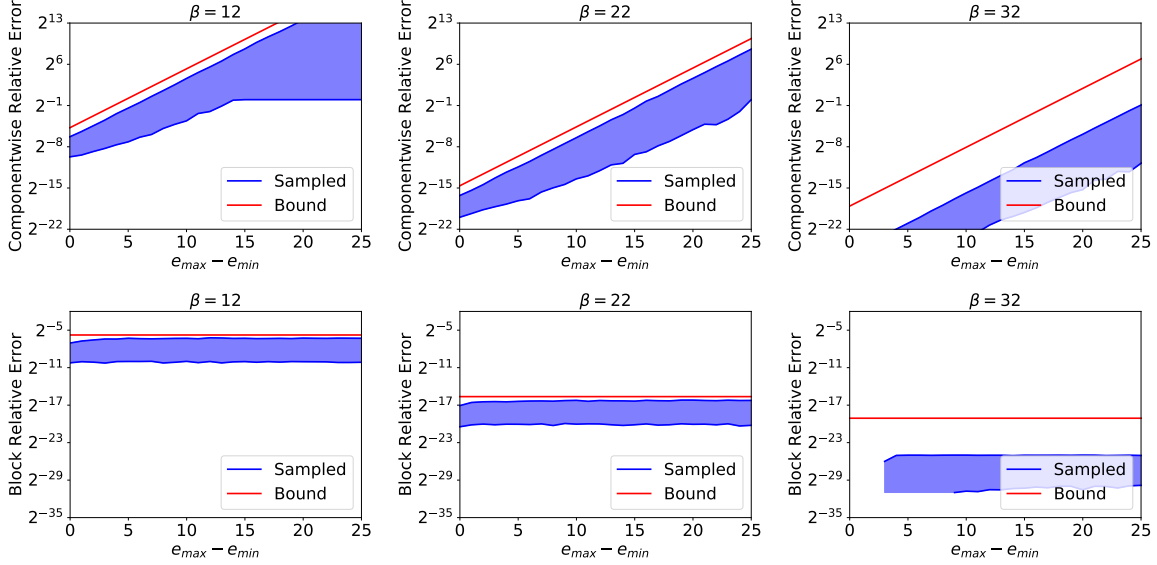


Fig. 5: 2-d Example with single precision: componentwise relative error (top) and block relative error (bottom) with respect to the difference in exponents ( $e_{max} - e_{min}$ ) for  $\beta \in \{12, 22, 32\}$ . The blue band represents the sampled maximum and minimum error and the red line depicts the theoretical bound.

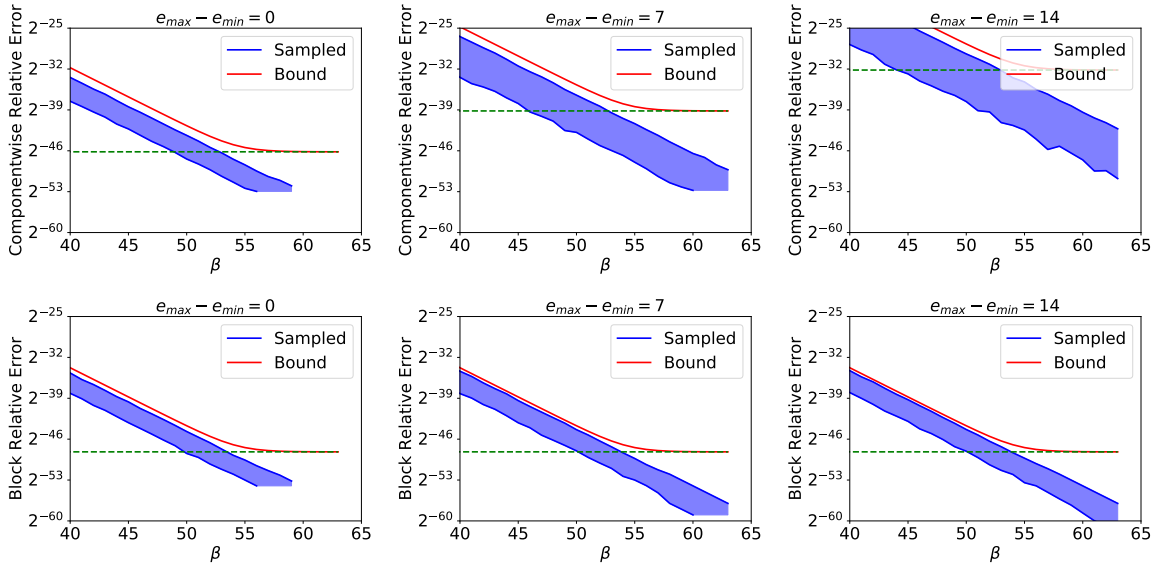


Fig. 6: 2-d Example with double precision: componentwise relative error (top) and block relative error (bottom) with respect to the precision parameter ( $\beta$ ) for  $e_{max} - e_{min} \in \{0, 7, 14\}$ . The blue band represents the sampled maximum and minimum error, the red line depicts the theoretical bound, and the dashed green line represents the asymptotic behavior of the theoretical bound.

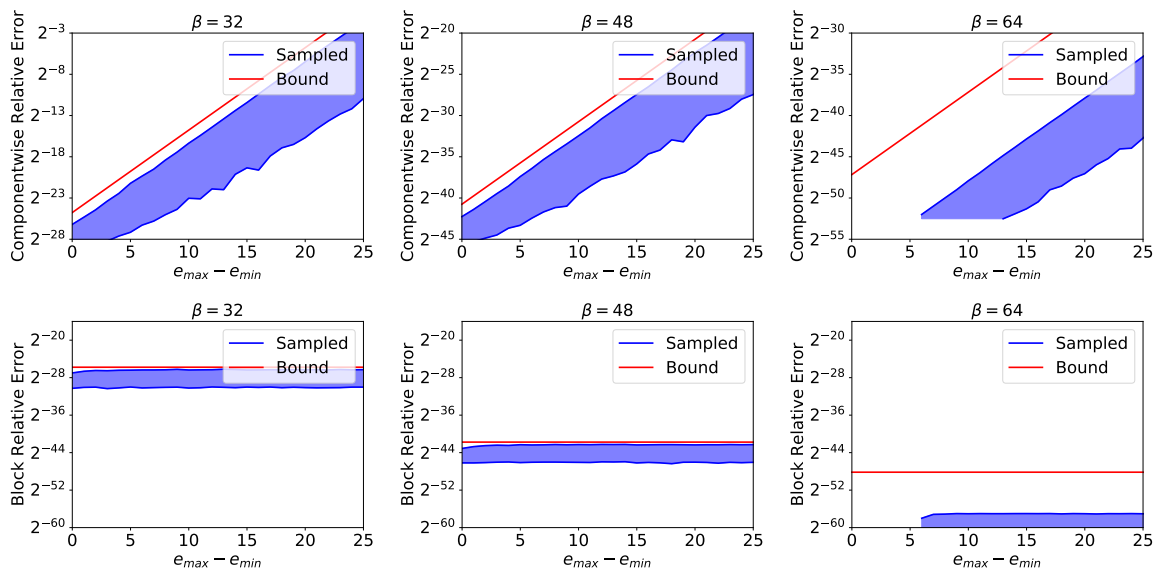


Fig. 7: 2-d Example with double precision: componentwise relative error (top) and block relative error (bottom) with respect to the difference in exponents ( $e_{max} - e_{min}$ ) for  $\beta \in \{32, 48, 64\}$ . The blue band represents the sampled maximum and minimum error and the red line depicts the theoretical bound.

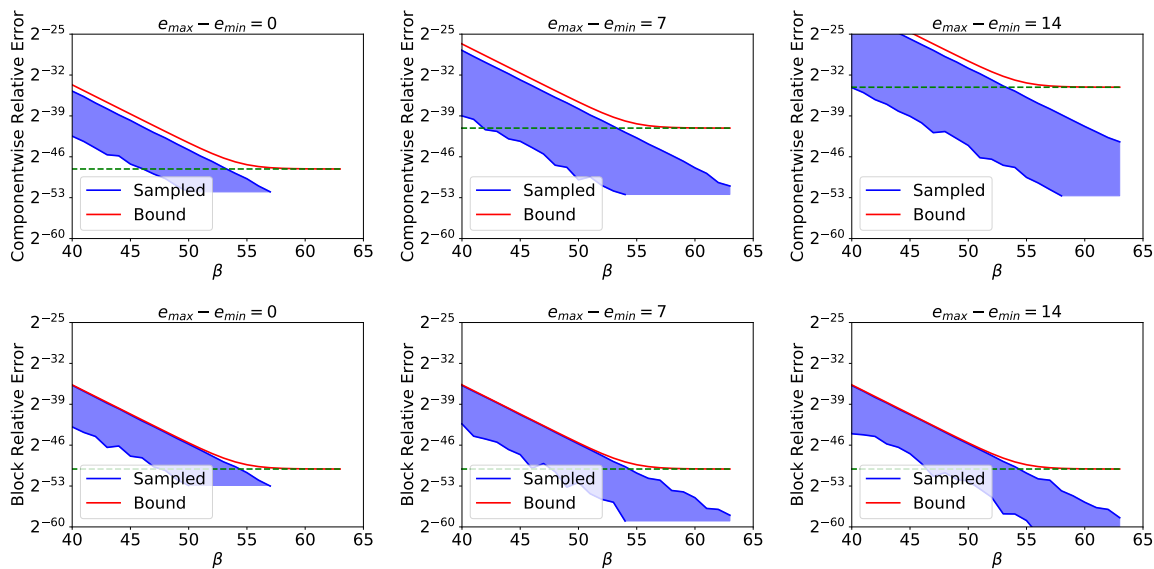


Fig. 8: 1-d Example with double precision: componentwise relative error (top) and block relative error (bottom) with respect to the precision parameter ( $\beta$ ) for  $e_{max} - e_{min} \in \{0, 7, 14\}$ . The blue band represents the sampled maximum and minimum error, the red line depicts the theoretical bound, and the dashed green line represents the asymptotic behavior of the theoretical bound.

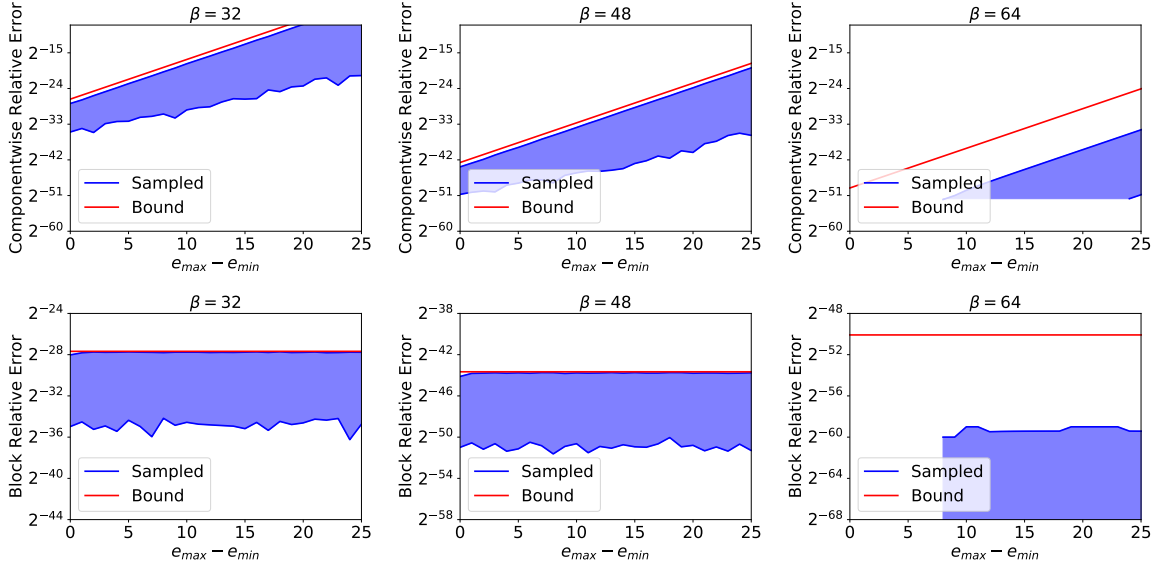


Fig. 9: 1-d Example with double precision: componentwise relative error (top) and block relative error (bottom) with respect to the difference in exponents ( $e_{max} - e_{min}$ ) for  $\beta \in \{32, 48, 64\}$ . The blue band represents the sampled maximum and minimum error and the red line depicts the theoretical bound.

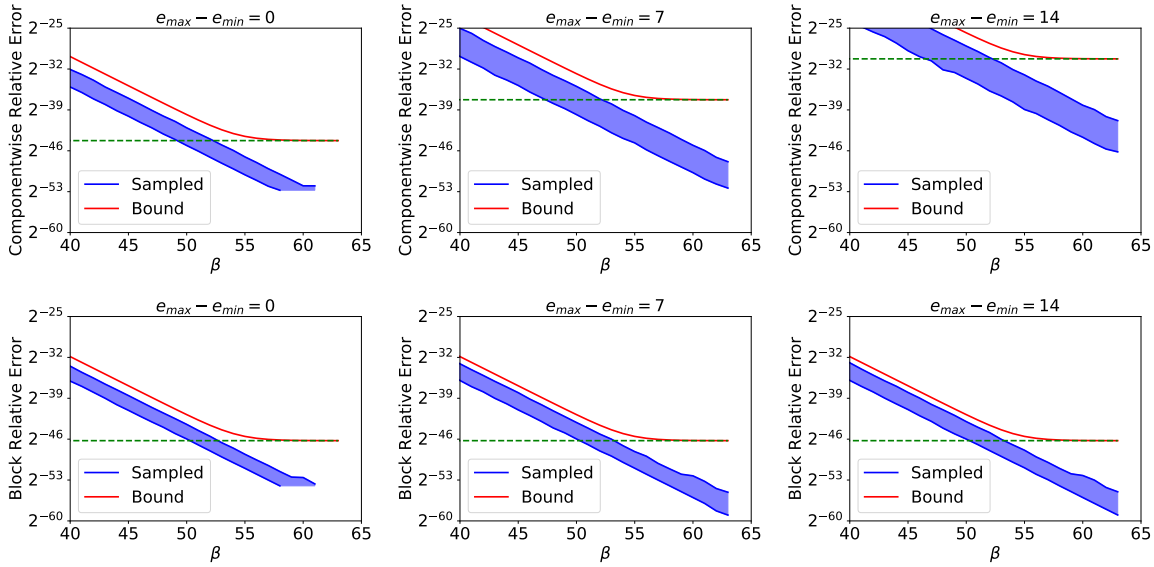


Fig. 10: 3-d Example with double precision: componentwise relative error (top) and block relative error (bottom) with respect to the precision parameter ( $\beta$ ) for  $e_{max} - e_{min} \in \{0, 7, 14\}$ . The blue band represents the sampled maximum and minimum of the error, the red line depicts the theoretical bound, and the dashed green line represents the asymptotic behavior of the theoretical bound.

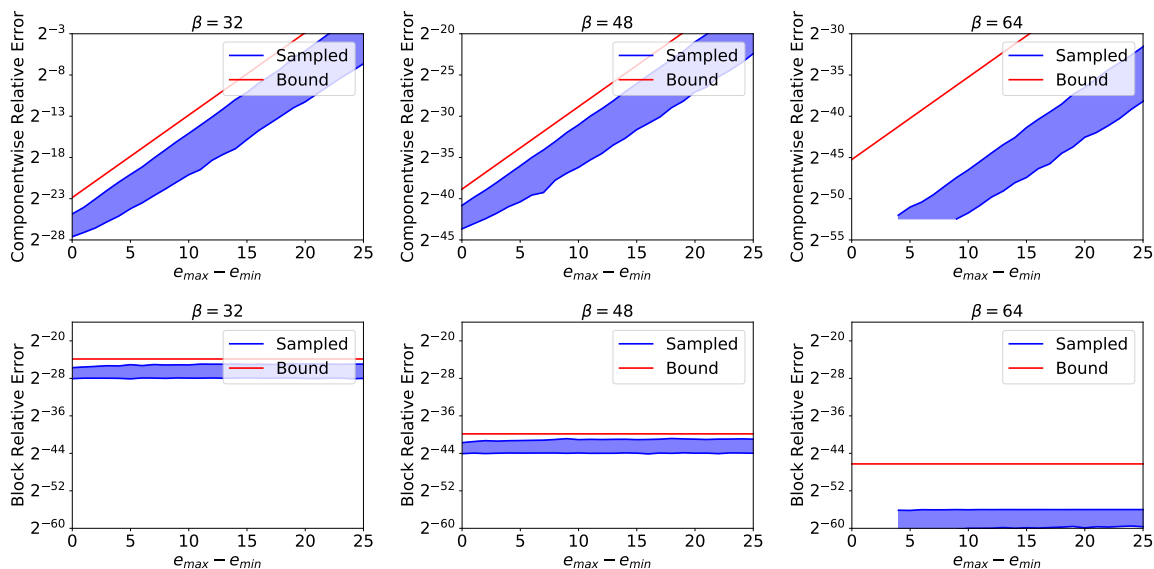


Fig. 11: 3-d Example with double precision: componentwise relative error (top) and block relative error (bottom) with respect to the difference in exponents ( $e_{max} - e_{min}$ ) for  $\beta = \{32, 48, 64\}$ . The blue band represents the sampled maximum and minimum of the error and the red line depicts the theoretical bound.

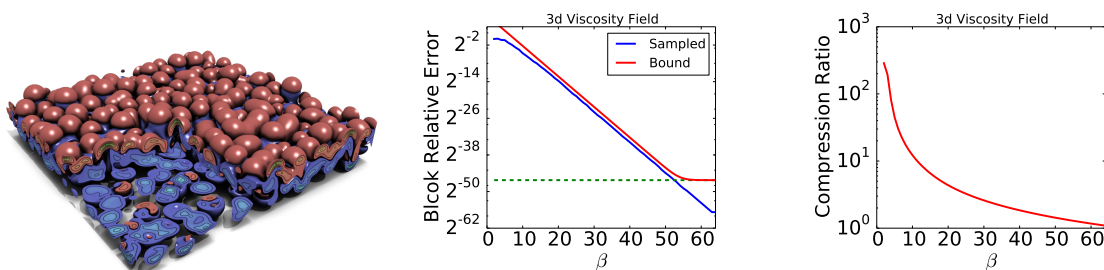


Fig. 12: 3-d viscosity field example with double precision. On the left is a 3-d rendering of the viscosity field. In the middle is the maximum block relative error as a function of the precision parameter  $\beta$ . The blue line is the error from ZFP compression and decompression with fixed  $\beta$  and the red line depicts the theoretical bound. On the right is the compression ratio as a function of  $\beta$ .

the true error for both examples. As for the compression ratio, since the density field has a smaller dynamic range, there is a substantial increase in the compression ratio for every bit plane removed, especially compared to the viscosity field. It can be concluded, that for some error tolerance, ZFP compresses at a higher ratio for data that is “smooth,” i.e., the exponent range for each block is small.

**7. Conclusion.** In this paper, we addressed the error introduced in the use of lossy compression of floating-point data. An important contribution of this paper is the formulation of the problem in a way that simplifies analysis. The vector space,  $\mathcal{B}^n$ , introduced in Section 3.1, proved to be useful in developing operators that accurately represent each step of the ZFP compression algorithm. Section 5 presented the error analysis of the current implementation of the fixed precision mode of ZFP



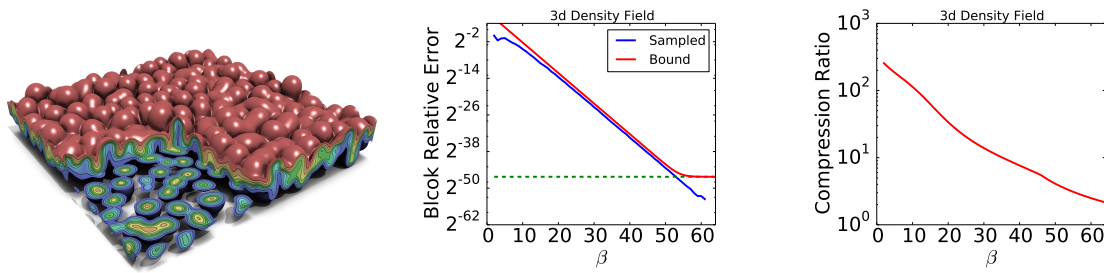


Fig. 13: 3-d density field example with double precision. On the left is a 3-d rendering of the density field. In the middle is the maximum block relative error as a function of the precision parameter  $\beta$ . The blue line is the error from ZFP compression and decompression with fixed  $\beta$  and the red line depicts the theoretical bound. On the right is the compression ratio as a function of  $\beta$ .

and the numerical tests presented in Section 6 provided a demonstration that the theoretical bounds established in this paper capture the error introduced by ZFP. The techniques presented in Section 3 and methodology from Sections 4 and 5 could be applied to any compression algorithm or numerical method involving direct manipulation of bits.

In the majority of mesh-based PDE simulations, it is reasonable to assume that most of the blocks provided as an input to the ZFP compression algorithm will be “smooth” in the sense that the exponent range,  $e_{max} - e_{min}$ , will be small and there will be some natural ordering correlation between the values within the block. As Theorem 5.2 represents the worst possible error achieved, the tests presented in Section 6.1 were constructed to provide an exposition of the worst case scenario (i.e., not “smooth”) of the error introduced by ZFP compression and decompression. Even so, the error bound established in Theorem 5.2 accurately, and narrowly, bounded the error in each example.

We limited our detailed analysis to the fixed precision implementation of ZFP, which is one of three possible compression modes implemented by ZFP. Using the bound in Theorem 5.2, we were able to provide a similar bound for the fixed accuracy and fixed rate modes. Further research is needed to determine a tighter error bound for the fixed rate mode for real-world data as most real-world problems will produce “smooth” values and the bound in Theorem 5.4 is for the worst case scenario.

Additionally, given the trends in computing hardware, methods are needed to reduce the memory capacity and bandwidth demands in simulation codes. One common technique is to use mixed precision algorithms, which typically require changing the underlying algorithms to achieve the same purpose. However, one technique with promise, particularly for grid-based PDE methods, is the use of lossy floating-point compression. In [16], the C++ compressed array primitives handle the complexity of decompression, caching, and compression transparently. By using ZFP instead, we can achieve bandwidth reduction without changing the underlying structure of the algorithm. An extension of our work would include an error analysis of the propagation of the errors of storing the solution state in compressed format for an iterative method, i.e., repeatedly decompressing and recompressing the solution data at each time step or iteration of the numerical algorithm.

Lastly, it should be noted that this paper has analyzed the error of converting an IEEE representation to ZFP. However, ZFP can be seen as a number representation itself, just like IEEE. Another interesting direction for future work would be to consider the behavior of round-off error of floating-point arithmetic conducted directly on the ZFP format.

**Appendix A. ZFP Toy Example.** Here we include a toy example of ZFP compression and decompression as implemented by the operators defined in Section 4. As the embedded coding implemented by ZFP in Step 7 is nontrivial and lossless we exclude it from the following example. More details on Step 7 can be found in the *Algorithm* section of [16]. As our analysis is focused on the fixed precision mode of ZFP and it is the simplest mode to illustrate, we only present the output for fixed precision mode at Step 8. Note that we will write  $x^{(i)}$  to denote the output from step  $i$  of ZFP.

*Compression:* We first outline the steps for compression on  $x = [5632, 3072, 400, 68]^T \in \mathbb{R}^4$ .

*Step 1:* As  $d = 1$  and the vector is already in  $\mathbb{R}^4$  there is no partitioning to be done.

*Step 2:* For simplicity, we will use  $k = 13$  and  $q = 9$ . First, as outlined in Section 4.2, the components are converted to a bit representation in  $\mathcal{B}$ . Next, we apply the shift operator  $S_\ell$  with  $\ell = e_{\max}(x) - q + 1 = 12 - 9 + 1 = 4$ . This operation amounts to shifting each bit four positions to the right. Finally, we apply the truncation operator  $T_{\mathcal{S}}$ , where  $\mathcal{S} = \{i \in \mathbb{Z} : i \geq 0\}$ . Hence, any bits after the decimal are dropped which will result in the loss of some information in this example. This procedure is illustrated below in (A.1). Note that the representations in (A.1) include the guard bit so they will have  $q + 1 = 10$  bits in their representation after the truncation phase. Additionally, there is one bit allotted for the sign bit which will not be represented below.

$$(A.1) \quad \begin{array}{c} \left[ \begin{array}{c} 5632 \\ 3072 \\ 400 \\ 68 \end{array} \right] \longrightarrow \left[ \begin{array}{c} 01011000000000 \\ 00110000000000 \\ 00000110010000 \\ 00000001000100 \end{array} \right] \longrightarrow \left[ \begin{array}{c} 0101100000.0000 \\ 0011000000.0000 \\ 0000011001.0000 \\ 0000000100.0100 \end{array} \right] \longrightarrow \left[ \begin{array}{c} 0101100000 \\ 0011000000 \\ 0000011001 \\ 0000000100 \end{array} \right] \\ \text{Decimal} \qquad \qquad \qquad \text{Signed Binary} \qquad \qquad \qquad \text{Bit Shift} \qquad \qquad \qquad x^{(2)} \end{array}$$

In addition to the bits used to store  $x^{(2)}$ , note that ZFP also encodes the value  $e_{\max}(x) = 12$ .

*Step 3:* Using Table 3 from Section 4.3, with  $\mathbf{a}_1 = 0101100000$ ,  $\mathbf{a}_2 = 0011000000$ ,  $\mathbf{a}_3 = 0000011001$ , and  $\mathbf{a}_4 = 0000000100$ , we can compute  $x^{(3)}$ . This process yields the vector

$$x^{(3)} = \begin{bmatrix} 0010001111 \\ 0001111000 \\ -0000100011 \\ 0000010011 \end{bmatrix}$$

and is outlined step by step below (steps work from left to right starting with upper left entry):

$\tilde{L}$			
$\mathbf{a}_1 \leftarrow \mathbf{a}_1 + \mathbf{a}_4$	$= 0101100100,$	$\mathbf{a}_1 \leftarrow r(\mathbf{a}_1)$	$= 0010110010,$
$\mathbf{a}_3 \leftarrow \mathbf{a}_3 + \mathbf{a}_2$	$= 0011011001,$	$\mathbf{a}_3 \leftarrow r(\mathbf{a}_3)$	$= 0001101100,$
$\mathbf{a}_1 \leftarrow \mathbf{a}_1 + \mathbf{a}_3$	$= 0100011110,$	$\mathbf{a}_1 \leftarrow r(\mathbf{a}_1)$	$= 0010001111,$
$\mathbf{a}_4 \leftarrow \mathbf{a}_4 + \mathbf{a}_2$	$= -0001011010,$	$\mathbf{a}_4 \leftarrow r(\mathbf{a}_4)$	$= -0000101101,$
$\mathbf{a}_4 \leftarrow \mathbf{a}_4 + r(\mathbf{a}_2)$	$= 0000010011,$	$\mathbf{a}_2 \leftarrow \mathbf{a}_2 - r(\mathbf{a}_4)$	$= 0001111000.$

*Step 4:* Note that the components of a vector in  $\mathbb{R}^4$  are already in total sequency order.

*Step 5:* The components are converted to a negabinary representation. Note that  $q + 2 = 11$  bits are available for the negabinary representation as it does not require a dedicated sign bit. Hence,

$$x^{(5)} = \begin{bmatrix} 00110010011 \\ 00110001000 \\ 00000101101 \\ 00000010111 \end{bmatrix}.$$

Negabinary

*Step 6:* The transposition is performed so that the first row corresponds to the most significant bit while the last row corresponds to the least significant bit. Hence  $x^{(6)} = (x^{(5)})^T$ . Note that the terminology *bit plane* used in the discussion of ZFP can be realized as the rows of bits in  $x^{(6)}$  or the columns of bits of  $x^{(5)}$ . For example, the third bit plane of  $x^{(6)}$  is 1100 and the sixth bit plane of  $x^{(6)}$  is 0010.

*Step 8:* Recall that we have decided to exclude Step 7 from this example for simplicity. In Step 8, the user provides a fixed number of bit planes,  $\beta$ , to keep from  $x^{(6)}$  starting with the most significant bit plane. The remaining bit planes are then ordered in a sequence as the rows of  $x^{(6)}$ . Supposing the number of bit planes to keep is  $\beta = 7$ , the output would be  $x^{(8)} = 0000\ 0000\ 1100\ 1100\ 0000\ 0010\ 1001$ . It should be noted that  $x^{(8)}$  is close to the compressed bit stream format of ZFP but is not in the exact compressed format since we did not perform Step 7. Note that if Step 7 had been performed then the final compressed bit sequence would have been 0 0 11110 110 000 00110 1011, requiring 6 fewer bits. This completes the steps for compression.

*Decompression:* We now highlight the steps for decompression. To decompress, we first convert the bit sequence back into a vector format and transpose. We then place zeros to the end of each row until we have the same number of bits before we dropped bit planes (in this case four zeros per row). This vector will be very similar to  $x^{(5)}$ , however, due to the removal of bit planes in Step 8 some information was lost that cannot be restored. Next, we convert each negabinary representation to a signed binary representation. These steps are illustrated in (A.2).

$$(A.2) \quad \begin{bmatrix} 0011001 \\ 0011000 \\ 0000010 \\ 0000001 \end{bmatrix} \longrightarrow \begin{bmatrix} 00110010000 \\ 00110000000 \\ 00000100000 \\ 00000010000 \end{bmatrix} \longrightarrow \begin{bmatrix} 0010010000 \\ 0010000000 \\ -0000100000 \\ 0000010000 \end{bmatrix}$$

Negabinary Signed Binary

We now use the final vector from (A.2) as the input for the routine outlined in Table 3 in Section 4.3.

$\tilde{L}^{-1}$					
$\mathbf{a}_2 \leftarrow \mathbf{a}_2 + r(\mathbf{a}_4) =$	0010001000,	$\mathbf{a}_4 \leftarrow \mathbf{a}_4 - r(\mathbf{a}_2) =$	-0000110100,		
$\mathbf{a}_2 \leftarrow \mathbf{a}_2 + \mathbf{a}_4 =$	0001010100,	$\mathbf{a}_4 \leftarrow s_{-1}(\mathbf{a}_4) =$	-0001101000, $\mathbf{a}_4 \leftarrow \mathbf{a}_4 - \mathbf{a}_2 =$	-0010111100,	
$\mathbf{a}_3 \leftarrow \mathbf{a}_3 + \mathbf{a}_1 =$	0001110000,	$\mathbf{a}_1 \leftarrow s_{-1}(\mathbf{a}_1) =$	0100100000,	$\mathbf{a}_1 \leftarrow \mathbf{a}_1 - \mathbf{a}_3 =$	0010110000,
$\mathbf{a}_2 \leftarrow \mathbf{a}_2 + \mathbf{a}_3 =$	0011000100,	$\mathbf{a}_3 \leftarrow s_{-1}(\mathbf{a}_3) =$	0011100000,	$\mathbf{a}_3 \leftarrow \mathbf{a}_3 - \mathbf{a}_2 =$	0000011100,
$\mathbf{a}_4 \leftarrow \mathbf{a}_4 + \mathbf{a}_1 =$	-0000001100,	$\mathbf{a}_1 \leftarrow s_{-1}(\mathbf{a}_1) =$	0101100000,	$\mathbf{a}_1 \leftarrow \mathbf{a}_1 - \mathbf{a}_4 =$	0101101100.

Lastly, we perform a bit shift of four bits to the left to undo the shift performed during Step 2 and convert to decimal to yield the decompressed vector. This procedure is illustrated below in (A.3).

$$(A.3) \quad \begin{bmatrix} 0101101100.0000 \\ 0011000100.0000 \\ 0000011100.0000 \\ -0000001100.0000 \end{bmatrix} \longrightarrow \begin{bmatrix} 01011011000000 \\ 00110001000000 \\ 00000111000000 \\ -00000011000000 \end{bmatrix} \longrightarrow \begin{bmatrix} 5824 \\ 3136 \\ 448 \\ -192 \end{bmatrix}$$

Signed Binary Bit Shift Decimal

We conclude by comparing the error with the bound in Theorem 5.2. Since  $d = 1$ ,  $k = 13$ ,  $q = 9$ , and  $\beta = 7$  for this example, we have that  $K_\beta \approx 0.19831$ . Since  $K_\beta \|x\|_\infty \leq (0.19832)(5632) \leq 1117$  and  $\|\tilde{D}\tilde{C}x - x\|_\infty = 260$  we observe that the bound established in Theorem 5.2 holds.

## Appendix B. Round-off Error of the Lossy Decorrelating Backwards Linear Transform.

There are three cases that must be considered: (i)  $\beta = q + 2$ , (ii)  $q - 2d + 2 < \beta < q + 2$ , and (iii)  $\beta \leq q - 2d + 2$ . We will investigate each separately in the following sections.

- (i) When  $\beta = q + 2$ , no information is lost at Step 8. Thus, from Table 3 we observe that the last two steps for the forward transform are exactly reversed by the first two steps of the backwards transform,

$$\begin{aligned} \tilde{L} \text{ Step 13 : } & \mathbf{a}_4 \leftarrow \mathbf{a}_4 + r(\mathbf{a}_2) \Rightarrow \mathbf{a}_4 = \mathbf{a}_4 + r(\mathbf{a}_2), \\ \tilde{L} \text{ Step 14 : } & \mathbf{a}_2 \leftarrow \mathbf{a}_2 - r(\mathbf{a}_4) \Rightarrow \mathbf{a}_2 = \mathbf{a}_2 - r(\mathbf{a}_4 + r(\mathbf{a}_2)), \\ \tilde{L}^{-1} \text{ Step 1 : } & \mathbf{a}_2 \leftarrow \mathbf{a}_2 + r(\mathbf{a}_4) \Rightarrow \mathbf{a}_2 = \mathbf{a}_2 - r(\mathbf{a}_4 + r(\mathbf{a}_2)) + r(\mathbf{a}_4 + r(\mathbf{a}_2)) = \mathbf{a}_2, \\ \tilde{L}^{-1} \text{ Step 2 : } & \mathbf{a}_4 \leftarrow \mathbf{a}_4 - r(\mathbf{a}_2) \Rightarrow \mathbf{a}_4 = (\mathbf{a}_4 + r(\mathbf{a}_2)) - r(\mathbf{a}_2) = \mathbf{a}_4. \end{aligned}$$

Thus, no error occurs by applying  $\tilde{L}_d^{-1}$ .

- (ii) If  $q - 2d + 2 < \beta < q + 2$ , then using similar techniques as for the forward linear transform operator, a bound can be found for the lossy backwards linear transform operator.

LEMMA B.1. *Suppose  $\mathbf{x} \in \mathbb{Z}^4$  such that  $e_{\max}(\mathbf{x}) = q - 1$ ,  $\mathbf{x} \neq \mathbf{0}$  and  $q - 2d + 2 < \beta < q + 2$ . Given the bit arithmetic implementation in Table 2 and Table 3 for ZFP's backwards linear transforms, we have*

$$\|L^{-1}\mathbf{x} - \tilde{L}^{-1}\mathbf{x}\|_\infty \leq \frac{5}{2}\epsilon_q\|\mathbf{x}\|_\infty \quad \text{and} \quad \|L_d^{-1}\mathbf{x} - \tilde{L}_d^{-1}\mathbf{x}\|_\infty \leq k_{L^{-1}}\epsilon_q\|\mathbf{x}\|_\infty,$$

where  $k_{L^{-1}} = \frac{5}{2}(2^d - 1)$ .

*Proof.* Use outline of proof from Lemma 4.3 and 4.4.  $\square$

- (iii) If  $\beta \leq q - 2d + 2$ , then the rightmost  $2d$  least significant bits of  $\mathbf{a}_i$  are zero, for all  $i$ , resulting in the following equivalences for the first two steps from Table 3:  $r(\mathbf{a}_4) = s_{-1}(\mathbf{a}_4)$ ,  $r(\mathbf{a}_2) = s_{-1}(\mathbf{a}_2)$ , and  $r(\mathbf{a}_4 + r(\mathbf{a}_2)) = s_{-1}(\mathbf{a}_4 + s_{-1}(\mathbf{a}_2))$ . Thus, the lossy backwards transform operator is exactly the lossless version, resulting in no additional error.

If  $q - 2d + 2 < \beta < q + 2$ , only a modest reduction of the data will be achieved over using  $\beta = q - 2d + 2$ . Thus, for the analysis of this paper, we chose to assume  $\beta \leq q - 2d + 2$  so that

$$\tilde{D}_3(\mathbf{a}) = D_3(\mathbf{a}) = F_B^{-1}L_d^{-1}F_B(\mathbf{a}), \text{ for all } \mathbf{a} \in \mathcal{B}^{4^d}.$$

Note, Theorem 5.2 can be modified to accommodate the error that occurs from the lossy backwards decorrelating operator.

THEOREM B.2. *Assume  $\mathbf{x} \in \mathbb{R}^{4^d}$  with  $\mathbf{x} \neq \mathbf{0}$  such that  $F_B(\mathbf{x}) \in \mathcal{B}_k^{4^d}$ , for some precision  $k$ . Let  $q - 2d + 2 < \beta < q + 2$  be the fixed precision parameter. Then*

$$(B.1) \quad \|\tilde{D}\tilde{C}\mathbf{x} - \mathbf{x}\|_\infty \leq B_\beta\|\mathbf{x}\|_\infty$$

where  $q \in \mathbb{N}$  is the precision for the block-floating point representation in Step 2,

$$(B.2) \quad B_\beta := k_{L^{-1}}\epsilon_q(1 + \epsilon_k) \left( \frac{8}{3}\epsilon_\beta + \epsilon_q \left( 1 + \frac{8}{3}\epsilon_\beta \right) (k_L(1 + \epsilon_q) + 1) \right) + K_\beta,$$

$k_L = \frac{7}{4}(2^d - 1)$ , and  $k_{L^{-1}} = \frac{5}{2}(2^d - 1)$ .

*Proof.* Use outline of proof from Theorem 5.2 along with Lemma B.1.  $\square$

**Appendix C. Discussion of error bound constant  $K_\beta$ .** First, note that  $K_\beta$  is a function of  $q$ ,  $k$ ,  $d$ , and  $\beta$ . Since  $k$  depends on the precision of the data provided to ZFP and  $d$  is the dimension of the input data it is important to note that two of the variables used in computing  $K_\beta$  are dependent

on the input data and cannot be changed by the user in ZFP. The value of  $q$  depends on the precision of data and is set to a value larger than  $k$ . For example, if the input values are IEEE single or double precision,  $q \in \{30, 62\}$ , since one bit is used to represent the sign bit and another to represent the overflow guard bit, as discussed in Section 4.2. The remaining variable,  $\beta$ , can be set to any positive integer when using the fixed precision mode of ZFP, as noted in Section 4.8. Figure 14 helps illustrate how  $K_\beta$  varies with respect to  $\beta$  and the dimensionality of the data,  $d$ . The lines on the contour plot in Figure 14 represent the log base 10 value of  $K_\beta$ , i.e.  $\log_{10}(K_\beta)$ . As suspected from the formula for  $K_\beta$ , we observe that a larger value of  $d$  has a greater effect on the value of  $K_\beta$  for small values of  $\beta$ .

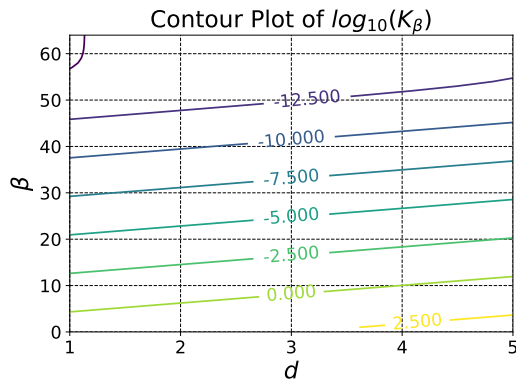


Fig. 14: Contour plot of  $\log_{10}(K_\beta)$  for  $\beta \in [1, 64]$  and dimension  $d \in [1, 5]$  with  $k = 53$  and  $q = 62$ .

#### REFERENCES

- [1] S. AHERN, A. SHOSHANI, K.-L. MA, A. CHOUDHARY, T. CRITCHLOW, S. KLASKY, V. PASCUCCHI, J. AHRENS, E. W. BETHEL, H. CHILDS, J. HUANG, K. JOY, Q. KOZIOL, G. LOFSTEAD, J. MERIFITH, K. MORELAND, G. OSTROUCHOV, M. PAPKA, V. VISHWANATH, M. WOLF, N. WRIGHT, AND K. WU, *Scientific Discovery at the Exascale: Report from the DOE ASCR 2011 Workshop on Exascale Data Management, Analysis, and Visualization*, tech. report, U.S. Department of Energy, Feb. 2011.
- [2] A. H. BAKER, D. M. HAMMERLING, S. A. MICKELSON, H. XU, M. B. STOLPE, P. NAVEAU, B. SANDERSON, I. EBERT-UPHOFF, S. SAMARASINGHE, F. DE SIMONE, F. CARBONE, C. N. GENCARELLI, J. M. DENNIS, J. E. KAY, AND P. LINDSTROM, *Evaluating lossy data compression on climate simulation data within a large ensemble*, *Geoscientific Model Development*, 9 (2016), pp. 4381–4403, <https://doi.org/10.5194/gmd-9-4381-2016>, <https://www.geosci-model-dev.net/9/4381/2016/>.
- [3] S. BORKAR AND A. A. CHIEN, *The future of microprocessors*, *CACM*, 54 (2011), pp. 67–77, <https://doi.org/10.1145/1941487.1941507>.
- [4] D. L. BROWN, P. MESSINA, D. KEYES, J. MORRISON, R. LUCAS, J. SHALF, P. BECKMAN, R. BRIGHTWELL, A. GEIST, J. VETTER, B. L. CHAMBERLAIN, E. LUSK, J. BELL, M. S. SHEPHARD, M. ANITESCU, D. ESTEP, B. HENDRICKSON, A. PINAR, AND M. A. HEROUX, *Scientific grand challenges: Crosscutting technologies for computing at the exascale*, tech. report, U.S. Department of Energy, Feb. 2010.
- [5] W. H. CABOT AND A. W. COOK, *Reynolds number effects on Rayleigh-Taylor instability with possible implications for Type Ia supernovae*, *Nature Physics*, 2 (2006), pp. 562 EP –, <http://dx.doi.org/10.1038/nphys361>.
- [6] R. H. DENNARD, F. H. GAENSSLEN, H. NIEN YU, V. L. RIDEOUT, E. BASSOUS, AND A. R. LEBLANC, *Design of ion-implanted MOSFET's with very small physical dimensions*, *Proceedings of the IEEE*, 87 (1999), pp. 668–678, <https://doi.org/10.1109/JPROC.1999.752522>.
- [7] L. P. DEUTSCH, *Deflate compressed data format specification version 1.3*, May 1996, <https://tools.ietf.org/html/rfc1951#section-Abstract> (accessed 2017-10-25).
- [8] S. DI AND F. CAPPELLO, *Fast error-bounded lossy HPC data compression with SZ*, in 2016 IEEE International Parallel and Distributed Processing Symposium (IPDPS), May 2016, pp. 730–739, <https://doi.org/10.1109/IPDPS.2016.11>.
- [9] N. HIGHAM, *Accuracy and Stability of Numerical Algorithms: Second Edition*, EngineeringPro collection, Society for Industrial and Applied Mathematics (SIAM, 3600 Market Street, Floor 6, Philadelphia, PA 19104), 2002, <https://books.google.com/books?id=7J52J4GrJKC>.

- [10] P. W. KATZ, *String searcher, and compressor using same*, Sept. 1991, [https://www.lens.org/lens/patent/US\\_5051745\\_A](https://www.lens.org/lens/patent/US_5051745_A).
- [11] D. E. KNUTH, *The Art of Computer Programming, Volume 2 (3rd Ed.): Seminumerical Algorithms*, Addison-Wesley Longman Publishing Co., Inc., Boston, MA, USA, 1997.
- [12] P. LANCASTER AND H. K. FARAHAT, *Norms on direct sums and tensor products*, *Mathematics of Computation*, 26 (1972), pp. 401–414, <http://www.jstor.org/stable/2005167>.
- [13] D. LANEY, S. LANGER, C. WEBER, P. LINDSTROM, AND A. WEGENER, *Assessing the effects of data compression in simulations using physically motivated metrics*, in *Proceedings of the International Conference on High Performance Computing, Networking, Storage and Analysis, SC '13*, New York, NY, USA, 2013, ACM, pp. 76:1–76:12, <https://doi.org/10.1145/2503210.2503283>, <http://doi.acm.org/10.1145/2503210.2503283>.
- [14] P. LINDSTROM, *Fixed-rate compressed floating-point arrays*, *IEEE Transactions on Visualization and Computer Graphics*, 20 (2014), pp. 2674–2683, <https://doi.org/10.1109/TVCG.2014.2346458>.
- [15] P. LINDSTROM, *Error distributions of lossy floating-point compressors*, *JSM Proceedings*, (2017), pp. 2574–2589.
- [16] P. LINDSTROM, *ZFP version 0.5.3*, April 2018. <https://zfp.readthedocs.io/en/release0.5.3/index.html>.
- [17] P. LINDSTROM AND M. ISENBURG, *Fast and efficient compression of floating-point data*, *IEEE Transactions on Visualization and Computer Graphics*, 12 (2006), pp. 1245–1250, <https://doi.org/10.1109/TVCG.2006.143>.
- [18] A. MITRA, *On finite wordlength properties of block-floating-point arithmetic*, *International Journal of Electrical, Computer, Energetic, Electronic and Communication Engineering*, 2 (2008).
- [19] K. R. RAO AND P. YIP, *Discrete Cosine Transform: Algorithms, Advantages, Applications*, Academic Press Professional, Inc., San Diego, CA, USA, 1990.
- [20] P. RATANAWORABHAN, J. KE, AND M. BURTSCHER, *Fast lossless compression of scientific floating-point data*, in *Proceedings of the Data Compression Conference, DCC '06*, Washington, DC, USA, 2006, IEEE Computer Society, pp. 133–142, <https://doi.org/10.1109/DCC.2006.35>, <https://doi.org/10.1109/DCC.2006.35>.
- [21] T. A. WELCH, *A technique for high-performance data compression*, *Computer*, 17 (1984), pp. 8–19, <https://doi.org/10.1109/MC.1984.1659158>.
- [22] S. WILLIAMS, A. WATERMAN, AND D. PATTERSON, *Roofline: An insightful visual performance model for multicore architectures*, *Commun. ACM*, 52 (2009), pp. 65–76, <https://doi.org/10.1145/1498765.1498785>, <http://doi.acm.org/10.1145/1498765.1498785>.
- [23] J. ZIV AND A. LEMPEL, *A universal algorithm for sequential data compression*, *IEEE Transactions on Information Theory*, 23 (1977), pp. 337–343, <https://doi.org/10.1109/TIT.1977.1055714>.
- [24] J. ZIV AND A. LEMPEL, *Compression of individual sequences via variable-rate coding*, *IEEE Transactions on Information Theory*, 24 (1978), pp. 530–536, <https://doi.org/10.1109/TIT.1978.1055934>.